

Novel Method for Multi-Dimensional Mapping of Higher Order Modulations for BICM-ID Over Rayleigh Fading Channels

Hassan M. Navazi and Md. Jahangir Hossain, *Member, IEEE*

The University of British Columbia, Kelowna, BC, Canada

hnavazi@alumni.ubc.ca, jahangir.hossain@ubc.ca

Abstract

Multi-dimensional (MD) mapping offers more flexibility in mapping design for bit-interleaved coded modulation with iterative decoding (BICM-ID) and potentially improves the bandwidth efficiency. However, for higher order signal constellations, finding suitable MD mappings is a very complicated task due to the large number of possible mappings. In this paper, a novel mapping method is introduced to construct efficient MD mappings to improve the error performance of BICM-ID over Rayleigh fading channels. We propose to break the MD mapping design problem into four distinct 2-D mapping functions. The 2-D mappings are designed such that the resulting MD mapping improves the BICM-ID error performance at low signal to noise ratios (SNRs). We also develop cost functions that can be optimized to improve the error performance at high SNRs. The proposed mapping method is very simple compared to well-known mapping methods, and it can achieve suitable MD mappings for different modulations including higher order modulations for BICM-ID. Simulation results show that our mappings significantly outperform the previously known mappings at a target bit error rate (BER) of 10^{-6} . Our mappings also offer a lower error-floor compared to their well-known counterparts.

Index Terms

BICM-ID, multi-dimensional signal mapping, QAM, Rayleigh fading channels.

I. INTRODUCTION

Trellis coded modulation (TCM) [1] improved the bit error rate (BER) performance of coded modulation by maximizing the Euclidean distance among the coded signal sequences. To improve the BER of TCM over Rayleigh fading channels, bit interleaved coded modulation (BICM) was introduced by Zehavi [2]. BICM offers good performance over Rayleigh fading channels. However, the random modulation caused by the interleaver degrades the BICM performance over additive white Gaussian noise (AWGN) channels. To address this problem, iterative decoding was used at the receiver. The resulting system is referred to as BICM with iterative decoding (BICM-ID) and is investigated in [3]-[5]. BICM-ID offers better performance over AWGN and Rayleigh fading channels. BICM can also use other iterative decoding schemes such as low density parity check code (LDPC). In [20], it is demonstrated that BICM-ID with signal space diversity (BICM-ID-SSD) outperforms the LDPC-BICM over fading channels. BICM-ID without SSD can also outperform LDPC-BICM when the number of iterations at the decoder is smaller than a certain number, which makes the decoder simpler. Moreover, compared to LDPC-BICM, BICM-ID uses a simple convolutional code instead of a more complex LDPC code. As such, BICM-ID offers a lower system complexity. Consequently, BICM-ID is a good candidate as a coded modulation especially when the system complexity becomes a more important concern.

It is widely known that the signal labeling map (mapping) plays a crucial role in BICM-ID performance[6]. Signal labeling is defined as the assignment of a binary sequence to a single symbol from a signal constellation. It is also referred to as multi-dimensional (MD) mapping when a sequence of binary bits is mapped to a vector of symbols instead of a single symbol. MD mapping is more flexible to design and also offers better bandwidth efficiency [7]. The MD labeling process is more adaptable to different design guidelines because MD space provides more diverse Euclidean distances among symbols. In [8], MD labeling was used for TCM and made the system's BER better through using the available bandwidth more efficiently. This development motivated researchers to use the MD labeling technique and its efficient use of bandwidth to further improve the BER of BICM-ID [7], [9]-[12]. The MD labeling technique can also be applied to higher order modulation to increase

the data rate of BICM-ID because using a larger constellation makes it possible to send more bits in the same signaling rate. However, providing a suitable MD labeling of a large constellation for BICM-ID is very challenging because of the large number of possible mappings. In general, for a $2N$ -D 2^m -ary modulation, there are $2^{mN}!$ possible mappings, where ! denotes the factorial operation. For example, the number of possible 4-D mappings for a 256-ary quadrature amplitude modulation (256-QAM) is 5.16×10^{287193} , which is an astronomical figure. It is important to note that MD mapping improves the performance of BICM-ID at a particular expense of the system's complexity [10]-[11]. However, the study of its complexity is beyond the scope of this paper.

Different labeling approaches for BICM-ID such as the genetic algorithm (GA), reactive tabu search (RTS) algorithm, extrinsic information transfer (EXIT)-based search algorithm, binary switching algorithm (BSA), and random labeling technique have been extensively investigated [6]-[25]. Indeed, high computational complexity is the main pitfall of all the proposed computer search based methods in the literature when looking for a good mapping of a large constellation.

The GA and RTS algorithms have been used in [14] and [15], respectively, to find the optimum mappings for BICM-ID. In these studies, however, the authors have not reported results for constellations larger than 64-QAM due to a very high computational complexity. In [16]-[19], an EXIT-based method is proposed to find suitable mappings that improve the iterative decoding systems BER at any signal to noise ratio (SNR) with an arbitrary number of iterations. In [20], the authors have designed an EXIT-chart aided search method to develop capacity approaching coded modulations. In particular, they have proposed a BICM-ID system with signal space diversity that approaches the channel capacity in both the fading and non-fading channels. However, the EXIT-based search considers both the modulator and encoder in detail and also the iterations between the decoder and demodulator. This makes the process complicated for finding a good mapping of a large MD constellation among a large number of possible labelings. The binary switching algorithm (BSA) [21], which is the best known mapping search method for BICM-ID, becomes intractable when searching for a good mapping of an MD constellation due to the huge search complexity [9],[11]. Although it is demonstrated in [9] and [13] that the random labeling technique results in

suitable mappings for BICM-ID, it is still computationally complex to look for a good mapping of a large constellation. This is because the random labeling method searches for a good mapping among a large set of randomly generated mappings. In addition to these computer search based methods, a heuristic method has also been explored in [12] to construct MD labeling for BICM-ID. But, this method is limited to 16- and 64-QAM. Moreover, this method is not designed for Rayleigh fading channels.

In this paper, we propose a novel method to develop suitable MD mappings to improve the BER performance of BICM-ID over Rayleigh fading channels in both the low and high SNR regions. To improve the BER performance of the system, we increase the harmonic mean of the minimum squared Euclidean distance (MSED) [6],[22] offered by the mapping.

The reported analytical and numerical results confirm the efficiency of the achieved mappings. The novelty and contributions of our work are as follows. (i) We break the MD labeling problem into four distinct 2-D mappings, which makes it easier to optimize the MD labeling. (ii) We design the four 2-D mappings such that the resulting MD mapping improves the BER of BICM-ID at low SNRs. (iii) We develop cost functions that can be optimized over the 2-D mappings to improve the performance of the resulting MD mapping's at high SNRs. (iv) We develop efficient MD mappings of higher order modulations including 2^m -ary ($m = 4, 5, \dots, 10$) modulations. Finally, (v) we propose efficient MD mappings of different modulation types including QAM, phase shift keying (PSK), and irregular modulations. Compared to the labeling method in [12], the proposed method in this paper has the following additional contributions. (i) The presemt study is not limited to a particular modulation type, i.e., it is not modulation spesific. However, the method in [12] is only for square QAMs. (ii) The proposed method in this paper can generate efficient mappings for modulations with different orders while the method in [12] is only for 16- and 64-ary particular modulations. (iii) Finally, the proposed method in this paper is designed specifically for Rayleigh fading channels. As a result, over fading channels, the resulting mappings outperform the mappings in [12].

The rest of this paper is organized as follows. The BICM-ID system model is described in Section II. The proposed MD labeling method is introduced in Section III. In Section IV, cost functions

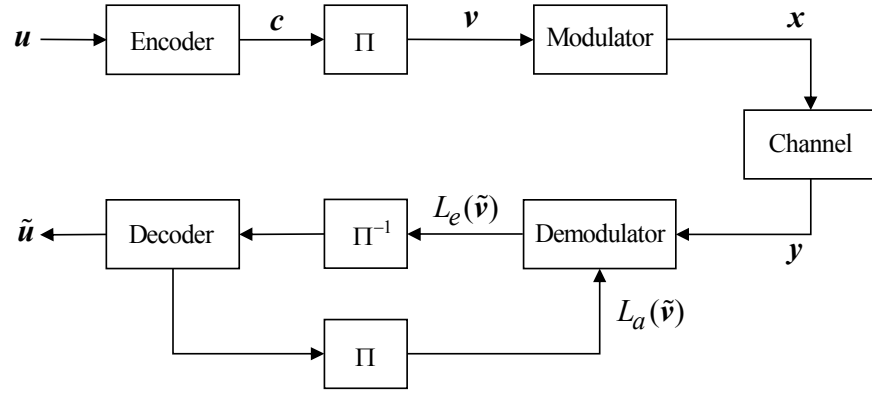


Fig. 1. The block diagram of a BICM-ID system.

are developed and optimized to obtain good MD mappings. Numerical results and discussions are presented in Section V. Finally, Section VI summarizes the conclusions.

II. SYSTEM MODEL

The block diagram of a conventional BICM-ID system is shown in Fig. 1. The transmitter is constructed from serial concatenation of a convolutional encoder, a bit interleaver and a modulator. In the system considered in this paper, the modulator maps a sequence of mN bits to a vector of N consecutive 2^m -ary signal points, using a MD mapping function $\mu : \{0, 1\}^{mN} \longrightarrow \chi = \chi^N$. Let $\mathbf{x} \in \chi$ be a $2N$ -D signal point represented as

$$\mathbf{x} = (x_1, x_2, \dots, x_N), \quad (1)$$

where $x_i \in \chi$. \mathbf{x} is labeled by an mN -bit binary sequence \mathbf{v} as

$$\mathbf{x} = \mu(\mathbf{v}). \quad (2)$$

The average energy per signal-vector is assumed to be 1, i.e., $E_{\mathbf{x}} = 1$. It is assumed that the channel state information is known at the receiver. The received signal-vector corresponding to the

transmitted signal-vector \mathbf{x} is given by

$$\mathbf{y} = h\mathbf{x} + \mathbf{n}, \quad (3)$$

where h is the Rayleigh fading coefficient corresponding to \mathbf{x} , and \mathbf{n} is a vector of N additive complex white Gaussian noise samples with zero-mean and variance N_0 . We assume that the fading coefficient for all signals in a signal-vector remains the same. Clearly, for the AWGN channels $h = 1$.

At the receiver, from the received signal y_t and the *a priori* log-likelihood ratio (LLR) of the coded bits, the demapper computes the *extrinsic* LLR for each of the bits in the received symbol as described in [4]. Then, the *extrinsic* LLRs are permuted by the random deinterleaver and used by the channel decoder. The decoder then calculates the *extrinsic* LLR on the coded bits using the BCJR algorithm [26]. These LLRs are interleaved and then fed back to the demapper to be used as the *a priori* LLRs in the next iteration.

III. PROPOSED MAPPING METHOD

As mentioned earlier, for a $2N$ -D 2^m -ary modulation there are $2^{mN}!$ possible mappings. In fact, a comprehensive computer search to find good mappings becomes intractable quickly as the modulation order increases. Even the well-known BSA mapping search method cannot be used directly to obtain good MD mappings of higher order modulations. Therefore, we propose an efficient technique to find good MD mappings for BICM-ID systems over Rayleigh fading channels.

A. Mapping Design Guideline

The performance of BICM-ID over Rayleigh fading channels is influenced by the *harmonic mean* of the MSED, which is calculated for a given mapping function, μ , applied to signal set χ . For a $2N$ -D mapping of a 2^m -ary constellation, the *harmonic mean* of the MSED is given by [10],[22]

$$\Phi(\mu, \chi) = \left(\frac{1}{mN2^{mN}} \sum_{i=1}^{mN} \sum_{b=0}^1 \sum_{\mathbf{x} \in \chi_b^i} \frac{1}{\|\mathbf{x} - \hat{\mathbf{x}}\|^2} \right)^{-1}, \quad (4)$$

where $\boldsymbol{x} = (x_1, x_2, \dots, x_N)$ is a $2N$ -D signal point and χ_b^i is the subset of signal points in χ whose labels take value b at the i^{th} bit position. For the performance in the low SNR region, $\hat{\boldsymbol{x}} = (\hat{x}_1, \hat{x}_2, \dots, \hat{x}_N)$ refers to the nearest neighbor¹ of \boldsymbol{x} in χ_b^i , and (4) is referred to as the harmonic mean of the MSED before feedback. For the asymptotic performance (performance in the high SNR region), χ_b^i involves only one symbol-vector $\hat{\boldsymbol{x}}$, which is different from \boldsymbol{x} only in the i^{th} bit position [22]. In this case, (4) is referred to as the harmonic mean of the MSED after feedback, which is denoted by $\hat{\Phi}(\mu, \chi)$. To achieve good performance in the low and high SNR regions, a large value of $\Phi(\mu, \chi)$ and $\hat{\Phi}(\mu, \chi)$ is required, respectively. However, maximizing (4) is a very complex problem even for a modulation such as 64-QAM [15]. We propose an innovative approach to generate MD mappings using 2-D mappings such that the resulting MD mapping has a greater value of $\Phi(\mu, \chi)$. Later, we develop cost functions that are optimized over the employed 2-D mappings to achieve a high value of $\hat{\Phi}(\mu, \chi)$ for the MD mapping. Our cost functions are very simple and give excellent results, even for higher order constellations such as MD 1024-QAM.

B. MD Mapping Using 2-D Mappings

Let $\boldsymbol{l} = (l_1, l_2, \dots, l_{mN})$ be an mN -bit binary label. We can write $\boldsymbol{l} = (\boldsymbol{l}_1, \boldsymbol{l}_2, \dots, \boldsymbol{l}_N)$, where \boldsymbol{l}_i is a m -bit binary label and is given by

$$\boldsymbol{l}_i = (l_{(i-1)m+1}, \dots, l_{im}); \quad i = 1, \dots, N. \quad (5)$$

Suppose that \mathcal{L} denotes the set of all mN -bit binary labels and \mathcal{L}_e and \mathcal{L}_o represent the subset of all $\boldsymbol{l} \in \mathcal{L}$ with even and odd Hamming weights, respectively. The MD mapping problem can be broken into four mappings in 2-D signal space as described below. According to the proposed MD mapping function, i.e., μ , label \boldsymbol{l} is mapped to the $2N$ -D signal point $\boldsymbol{x} = (x_1, \dots, x_N)$ as given below

¹The symbol-vectors with the minimum Euclidean distance are referred to as the nearest neighbours.

$$x_i = \begin{cases} \lambda_{el}(\mathbf{l}_i) & \text{if } i = 1, \mathbf{l} \in \mathcal{L}_e, \\ \lambda_{ol}(\mathbf{l}_i) & \text{if } i = 1, \mathbf{l} \in \mathcal{L}_o, \\ \lambda_{er}(\mathbf{l}_i) & \text{if } i \geq 2, \mathbf{l} \in \mathcal{L}_e, \\ \lambda_{or}(\mathbf{l}_i) & \text{if } i \geq 2, \mathbf{l} \in \mathcal{L}_o, \end{cases}; \quad i = 1, \dots, N, \quad (6)$$

where λ_{el} , λ_{ol} , λ_{er} , and λ_{or} are 2-D mapping functions, which will be discussed later in this section. In the applied mapping, let χ_e and χ_o represent the subset of signal points in χ whose labels belong to \mathcal{L}_e and \mathcal{L}_o , respectively. Without loss of generality, assume that $\mathbf{x} \in \chi_e$ and $\hat{\mathbf{x}} \in \chi_o$ where $\hat{\mathbf{x}} = (\hat{x}_1, \hat{x}_2, \dots, \hat{x}_N)$ is a signal point whose label is different from that of \mathbf{x} only in one bit position. We partition the 2-D signal constellation χ into two separate subsets with equal cardinalities and denote them as χ_{el} and χ_{ol} . Then, we limit the first element in \mathbf{x} and $\hat{\mathbf{x}}$, i.e., x_1 and \hat{x}_1 , to belong to χ_{el} and χ_{ol} , respectively. In (6), $\lambda_{el}(\cdot)$ and $\lambda_{ol}(\cdot)$ each map an m -bit label to a 2-D signal point chosen from χ_{el} and χ_{ol} , respectively. However, χ_{el} and χ_{ol} involve only 2^{m-1} signal points while there are 2^m distinct m -bit labels. As a consequence, each signal point in χ_{el} and χ_{ol} should be mapped by two m -bit labels simultaneously. In order to obtain a one-to-one MD mapping function, we restrict the two labels that are mapped to a particular signal point in either χ_{el} or χ_{ol} to be different in an odd number of bits. Specifically, we assume they are different only in the first bit position. This prohibits the labels with a Hamming distance larger than $(m + 1)$ bits to be mapped to the nearest neighbours in either of χ_e or χ_o . As a result, the value of $\Phi(\mu, \chi)$ increases. On the other hand, there is no constraint on $\lambda_{er}(\cdot)$ and $\lambda_{or}(\cdot)$ except they need to be bijective.

Proposition 1. *Let us assume that $\mathbf{l}_1 = (l_1^1, l_1^2, \dots, l_1^n)$ and $\mathbf{l}_2 = (l_2^1, l_2^2, \dots, l_2^n)$ are two n -bit labels, $D = d_H(\mathbf{l}_1, \mathbf{l}_2)$ is the Hamming distance between \mathbf{l}_1 and \mathbf{l}_2 , and $W = w_1 + w_2$, where w_j is the Hamming weight of \mathbf{l}_j ($j = 1, 2$). If $W \in \mathbb{E}$, $D \in \mathbb{E}$, and if $W \in \mathbb{E}$, $D \in \mathbb{E}$.*

Proof. See Appendix A. □

Proposition 2. *In the proposed MD mapping function, μ , there is a one-to-one correspondence*

between MD signal points and binary labels.

Proof. See Appendix B.

□

Proposition 3. *In the proposed MD mapping function, the Hamming distance between the nearest neighbours in either of χ_e or χ_o cannot be larger than $(m + 1)$ bits.*

Proof. See Appendix C.

□

IV. DEVELOPMENT AND OPTIMIZATION OF COST FUNCTIONS TO IMPROVE $\hat{\Phi}$

As mentioned in Section III-A, maximizing the harmonic mean is a very complicated task. In this section, we use the 2-D mappings in (6), i.e., λ_{el} , λ_{ol} , λ_{er} , λ_{or} , to develop two cost functions and derive a lower bound for $\hat{\Phi}(\mu, \chi)$, i.e., Δ . Then, we propose an algorithm to maximize Δ by optimizing the cost functions over the 2-D mappings. As such, the achieved 2-D mappings construct a MD mapping that provides a larger value of Δ , which results in a larger value of $\hat{\Phi}(\mu, \chi)$.

A. Development of Cost Functions

In order to achieve a lower bound for $\hat{\Phi}(\mu, \chi)$, Δ , we develop an upper bound for $\hat{\Phi}(\mu, \chi)^{-1}$. In particular, we first decompose $\hat{\Phi}^{-1}$ into two equal parts, i.e., $\Omega_e(\mu, \chi)$ and $\Omega_o(\mu, \chi)$, where in Ω_e , $x \in \chi_e$ and $\hat{x} \in \chi_o$. Next, we derive an upper bound for $\Omega_e(\mu, \chi)$, i.e., $\Psi(\mu, \chi)$, and then, we decompose Ψ into $\Psi_l(\mu, \chi)$ and $\Psi_r(\mu, \chi)$, where Ψ_l uses only the first symbol in x and \hat{x} , i.e., x_1 and \hat{x}_1 , and Ψ_l uses the rest of symbols in x and \hat{x} . As $x \in \chi_e$ and $\hat{x} \in \chi_o$, x_1 and \hat{x}_1 in Ψ_l are obtained using the mapping functions λ_{el} and λ_{ol} , respectively, while x_i and \hat{x}_i ($2 \leq i \leq N$) in Ψ_r are obtained using λ_{er} and λ_{or} , respectively. Thus, we develop two cost functions ψ_l and ψ_r , where ψ_l generates the same values as Ψ_l by considering all the cases of using λ_{el} and λ_{ol} in Ψ_l , and ψ_r generates the same values as Ψ_r by considering all the cases of using λ_{er} and λ_{or} in Ψ_r . Finally, we use ψ_l and ψ_r to develop Δ . In what follows, we discuss these steps in more detail.

We use (4) to write

$$\hat{\Phi}(\mu, \chi)^{-1} = \Omega_e(\mu, \chi) + \Omega_o(\mu, \chi), \quad (7)$$

where

$$\Omega_e(\mu, \chi) = \frac{1}{mN2^{mN}} \sum_{i=1}^{mN} \sum_{b=0}^1 \sum_{\substack{\mathbf{x} \in \chi_b^i \\ \mathbf{x} \in \chi_e}} \frac{1}{\|\mathbf{x} - \hat{\mathbf{x}}\|^2} \quad (8)$$

and

$$\Omega_o(\mu, \chi) = \frac{1}{mN2^{mN}} \sum_{i=1}^{mN} \sum_{b=0}^1 \sum_{\substack{\mathbf{x} \in \chi_b^i \\ \mathbf{x} \in \chi_o}} \frac{1}{\|\mathbf{x} - \hat{\mathbf{x}}\|^2}. \quad (9)$$

The sets χ_e and χ_o have the same cardinality. Moreover, when a given \mathbf{x} is in χ_e then the corresponding $\hat{\mathbf{x}}$ belongs to χ_o and vice versa. Therefore, (8) and (9) use the same set of Euclidean distances, which results in $\Omega_e(\mu, \chi) = \Omega_o(\mu, \chi)$. As a result, using (7) we have

$$\hat{\Phi}(\mu, \chi)^{-1} = 2\Omega_e(\mu, \chi). \quad (10)$$

Since $\|\mathbf{x} - \hat{\mathbf{x}}\|^2 = \sum_{j=1}^N |x_j - \hat{x}_j|^2$, then (8) can be rewritten as

$$\Omega_e(\mu, \chi) = \frac{1}{mN2^{mN}} \sum_{i=1}^{mN} \sum_{b=0}^1 \sum_{\substack{\mathbf{x} \in \chi_b^i \\ \mathbf{x} \in \chi_e}} \frac{1}{\sum_{j=1}^N |x_j - \hat{x}_j|^2}. \quad (11)$$

Proposition 4. Let $\mathbf{y} = (y_1, y_2, \dots, y_N)$ be a vector of non-negative real numbers. Then, we have

$$\frac{1}{\sum_{i=1}^N y_i} \leq \frac{1}{N} \sum_{j=1}^N \frac{1}{y_j}. \quad (12)$$

Proof. See Appendix D. □

Applying (12) in (11), we can write

$$\Omega_e(\mu, \chi) \leq K\Psi(\mu, \chi) \quad (13)$$

where $K = \frac{1}{mN^2 2^{mN}}$ is a constant value and $\Psi(\mu, \chi)$ is defined as

$$\Psi(\mu, \chi) = \sum_{i=1}^{mN} \sum_{b=0}^1 \sum_{\substack{\mathbf{x} \in \mathcal{X}_b^i \\ \mathbf{x} \in \mathcal{X}_e}} \sum_{j=1}^N \frac{1}{|x_j - \hat{x}_j|^2}.$$

We can decompose $\Psi(\mu, \chi)$ as

$$\Psi(\mu, \chi) = \Psi_l(\mu, \chi) + \Psi_r(\mu, \chi), \quad (14)$$

where $\Psi_l(\mu, \chi)$ and $\Psi_r(\mu, \chi)$ are given by

$$\Psi_l(\mu, \chi) = \sum_{i=1}^{mN} \sum_{b=0}^1 \sum_{\substack{\mathbf{x} \in \mathcal{X}_b^i \\ \mathbf{x} \in \mathcal{X}_e}} \frac{1}{|x_1 - \hat{x}_1|^2} \quad (15)$$

and

$$\Psi_r(\mu, \chi) = \sum_{i=1}^{mN} \sum_{b=0}^1 \sum_{\substack{\mathbf{x} \in \mathcal{X}_b^i \\ \mathbf{x} \in \mathcal{X}_e}} \sum_{j=2}^N \frac{1}{|x_j - \hat{x}_j|^2}. \quad (16)$$

Let $\mathbf{l} = (l_1, l_2, \dots, l_{mN})$ and $\hat{\mathbf{l}} = (\hat{l}_1, \hat{l}_2, \dots, \hat{l}_{mN})$ are two mN -bit labels, which are different only in the i^{th} bit position, and are mapped to $\mathbf{x} = (x_1, \dots, x_N)$ and $\hat{\mathbf{x}} = (\hat{x}_1, \dots, \hat{x}_N)$, respectively. We define \mathbf{l}_i and $\tilde{\mathbf{l}}_i$ respectively as the i^{th} m -tuple bits of \mathbf{l} and $\hat{\mathbf{l}}$, and rewrite $\mathbf{l} = (l_1, l_2, \dots, l_{mN})$ and $\tilde{\mathbf{l}} = (\tilde{l}_1, \tilde{l}_2, \dots, \tilde{l}_{mN})$. Then, Ψ_l in (15) is equal to Ψ'_l , which is given by

$$\Psi'_l(\lambda_{el}, \lambda_{ol}, \mathcal{L}) = \sum_{i=1}^{mN} \sum_{b=0}^1 \sum_{\substack{\mathbf{l} \in \mathcal{L}_b^i \\ \mathbf{l} \in \mathcal{L}_e}} \frac{1}{|\lambda_{el}(\mathbf{l}_1) - \lambda_{ol}(\hat{\mathbf{l}}_1)|^2}, \quad (17)$$

where $\mathcal{L}_b^i \in \mathcal{L}$ is the subset of labels with value b in their i^{th} bit position. For a given m -bit sequence \mathbf{l}_i , $\hat{\mathbf{l}}_i$ can take $(m+1)$ distinct m -bit sequences, where each one is the same as \mathbf{l}_i or different from \mathbf{l}_i only in one bit position. For example, if $m = 4$ and $\mathbf{l}_i = (0, 0, 0, 0)$, $\hat{\mathbf{l}}_i$ can take either of the 5 labels in $\{(0, 0, 0, 0), (0, 0, 0, 1), (0, 0, 1, 0), (0, 1, 0, 0), (1, 0, 0, 0)\}$. Let $\boldsymbol{\alpha} = (\alpha_1, \dots, \alpha_m)$ and $\boldsymbol{\beta} = (\beta_1, \dots, \beta_m)$ be two binary sequences, where $\boldsymbol{\beta}$ has the Hamming distance of either zero or

one bit from $\boldsymbol{\alpha}$. The set of $(m+1)$ possibilities for $\boldsymbol{\beta}$ is denoted by \mathcal{B} . Assume that for a given i , $\mathbf{l}_i = \boldsymbol{\alpha}$ and $\hat{\mathbf{l}}_i = \boldsymbol{\beta}$. Then, Ψ'_l in (17) is equal to ψ_l , which is defined as

$$\psi_l(\lambda_{el}, \lambda_{ol}, \chi_{el}, \chi) = \sum_{\boldsymbol{\alpha}} \sum_{\boldsymbol{\beta} \in \mathcal{B}} \frac{a_{\boldsymbol{\alpha}, \boldsymbol{\beta}}^{(l)}}{|\lambda_{el}(\boldsymbol{\alpha}) - \lambda_{ol}(\boldsymbol{\beta})|^2}, \quad (18)$$

where $a_{\boldsymbol{\alpha}, \boldsymbol{\beta}}^{(l)}$ is computed as

$$a_{\boldsymbol{\alpha}, \boldsymbol{\beta}}^{(l)} = \sum_{i=1}^{mN} \sum_{b=0}^1 \sum_{\substack{\mathbf{l} \in \mathcal{L}_b^i \\ \mathbf{l} \in \mathcal{L}_e}} I(\mathbf{l}_1 = \boldsymbol{\alpha}, \hat{\mathbf{l}}_1 = \boldsymbol{\beta}), \quad (19)$$

where $I(x)$ is an indicator function and is defined as

$$I(x) = \begin{cases} 1, & \text{if } x \text{ is true,} \\ 0, & \text{otherwise.} \end{cases} \quad (20)$$

Similarly, Ψ_r in (16) is equal to Ψ'_r , which is given by

$$\Psi'_r(\lambda_{er}, \lambda_{or}, \mathcal{L}) = \sum_{i=1}^{mN} \sum_{b=0}^1 \sum_{\substack{\mathbf{l} \in \mathcal{L}_b^i \\ \mathbf{l} \in \mathcal{L}_e}} \sum_{j=2}^N \frac{1}{|\lambda_{er}(\mathbf{l}_j) - \lambda_{or}(\hat{\mathbf{l}}_j)|^2}. \quad (21)$$

The m -bit elements \mathbf{l}_i in $\mathbf{l} = (\mathbf{l}_1, \mathbf{l}_2, \dots, \mathbf{l}_N)$ are independent from one another for all values of i .

Then, Ψ'_r in (21) is equal to ψ_r , which is defined as

$$\psi_r(\lambda_{er}, \lambda_{or}, \chi) = \sum_{i=1}^{mN} \sum_{b=0}^1 \sum_{\substack{\mathbf{l} \in \mathcal{L}_b^i \\ \mathbf{l} \in \mathcal{L}_e}} \frac{N-1}{|\lambda_{er}(\mathbf{l}_2) - \lambda_{or}(\hat{\mathbf{l}}_2)|^2}, \quad (22)$$

and can be rewritten as

$$\psi_r(\lambda_{er}, \lambda_{or}, \chi) = \sum_{\boldsymbol{\alpha}} \sum_{\boldsymbol{\beta} \in \mathcal{B}} \frac{(N-1)a_{\boldsymbol{\alpha}, \boldsymbol{\beta}}^{(r)}}{|\lambda_{er}(\boldsymbol{\alpha}) - \lambda_{or}(\boldsymbol{\beta})|^2}, \quad (23)$$

where $a_{\alpha,\beta}^{(r)}$ is computed as

$$a_{\alpha,\beta}^{(r)} = \sum_{i=1}^{mN} \sum_{b=0}^1 \sum_{\substack{l \in \mathcal{L}_b^i \\ l \in \mathcal{L}_e}} I(l_2 = \alpha, \hat{l}_2 = \beta). \quad (24)$$

Using (10), (13), and (14), a lower bound of $\hat{\Phi}(\mu, \chi)$ can be derived as follows

$$\begin{aligned} \hat{\Phi}^{-1}(\mu, \chi) &\leqslant 2K (\Psi_l(\mu, \chi) + \Psi_r(\mu, \chi)) \\ &\Rightarrow \Delta \leqslant \hat{\Phi}(\mu, \chi), \end{aligned} \quad (25)$$

where Δ is given by

$$\Delta = \frac{1}{2K(\Psi_l(\mu, \chi) + \Psi_r(\mu, \chi))}. \quad (26)$$

Because $\Psi_l(\mu, \chi) = \psi_l(\lambda_{el}, \lambda_{ol}, \chi_{el}, \chi)$ and $\Psi_r(\mu, \chi) = \psi_r(\lambda_{er}, \lambda_{or}, \chi)$, we rewrite Δ as

$$\Delta = \frac{1}{2K(\psi_l(\lambda_{el}, \lambda_{ol}, \chi_{el}, \chi) + \psi_r(\lambda_{er}, \lambda_{or}, \chi))}. \quad (27)$$

Note that (27) operates in 2-D signal space rather than MD signal space, and as a result, optimization is much simpler.

Our objective is to maximize Δ and then to calculate the corresponding $\hat{\Phi}(\mu, \chi)$. Since $\psi_l(\lambda_{el}, \lambda_{ol}, \chi_{el}, \chi)$ and $\psi_r(\lambda_{er}, \lambda_{or}, \chi)$ are independent from each other, then the maximum value of Δ , Δ_{max} , is given by

$$\Delta_{max} = \frac{1}{2K} \left[\min_{\lambda_{el}, \lambda_{ol}, \chi_{el}} \psi_l(\lambda_{el}, \lambda_{ol}, \chi_{el}, \chi) + \min_{\lambda_{er}, \lambda_{or}} \psi_r(\lambda_{er}, \lambda_{or}, \chi) \right]^{-1}. \quad (28)$$

B. Minimization of Cost Functions

The minimization of the cost functions ψ_l and ψ_r in (28) can be done using the BSA [21]. Note that the minimization of ψ_r is simpler than that of ψ_l because ψ_r deals with fewer effective arguments. Thus, we first optimize ψ_r , and then, use the obtained results to simplify the minimization of ψ_l .

1) *Minimization of ψ_r* : To minimize ψ_r , two random mappings are initially considered as λ_{er} and λ_{or} . Then, the BSA is used to minimize ψ_r by modifying λ_{er} and λ_{or} . In fact in ψ_r , the cost value for a given symbol in λ_{er} is computed by using $(m + 1)$ corresponding symbols from λ_{or} . As a result, simultaneously modifying λ_{er} and λ_{or} can make the optimization complex. Therefore, our approach is to minimize ψ_r by alternately modifying each of λ_{er} and λ_{or} . In other words, we use the BSA to decrease ψ_r by modifying λ_{er} . After a given number of iterations, λ_{er} and λ_{or} are exchanged. Again, the BSA is used to decrease ψ_r by modifying the new λ_{er} . This procedure is repeated up to a given number of iterations.

2) *Minimization of ψ_l* : In addition to λ_{el} and λ_{ol} , χ_{el} is another effective argument in computing ψ_l . As there is no constraint on χ_{el} , it is a complex process to minimize ψ_l . To simplify the optimization process, χ_{el} is constrained to involve only the symbols whose labels in the obtained λ_{er} take binary value b in a given bit position. In this paper, we assume that χ_{el} involves the symbols whose labels in λ_{er} take the value zero in the first bit-position. The functions ψ_l and ψ_r are computed by considering the similar Euclidean distances between two-dimensional symbols. As a result, there is a potential advantage in applying the above mentioned constraint on χ_{el} because it will be easier to find a suitable λ_{el} corresponding to a given λ_{ol} . After determining χ_{el} and χ_{ol} , two random mappings are generated as λ_{el} and λ_{ol} . Again the BSA is applied to minimize ψ_l by modifying λ_{el} . Then, λ_{el} is exchanged by λ_{ol} and the BSA minimizes ψ_l by modifying the new λ_{el} . This procedure is repeated up to a given number of iterations.

By executing the proposed algorithm for a certain number of iterations, a local maximum value is calculated using (28). The search algorithm is executed several times and each time the corresponding value for $\hat{\Phi}(\mu, \chi)$ is calculated. Finally, the modulations corresponding to the maximum obtained $\hat{\Phi}(\mu, \chi)$ are chosen. Fig. 2 illustrates the flowchart of the proposed algorithm. Numerical results confirm that the proposed algorithm generates mappings with significantly large values of $\hat{\Phi}(\mu, \chi)$. As a result, the obtained mappings would also improve the error performance of BICM-ID systems in the high SNR region over Rayleigh fading channels.

C. Simplified BSA

We use the simplified BSA in our algorithm to reduce the search complexity. The BSA calculates a cost function for each symbol in an initial random mapping, and then, lists the symbols in descending order in terms of cost value. Next, the label of the symbol with the highest cost value is switched with the label of another symbol such that the total cost is reduced as much as possible. After each switch, the BSA again lists the symbols in descending cost value and repeats the switching process. It is important to note that each switch in the subsequent rounds of the BSA affects the cost value of only a limited number of symbols in the mapping. In particular, in maximizing $\hat{\Phi}(\mu, \chi)$ for a given modulation using the BSA, when the label of symbol s_i , i.e., l_i , is switched by label of symbol s_j , i.e., l_j , the cost value changes only for s_i and s_j and for the symbols whose labels are different from l_i or l_j only in one bit position. For example, for a 2^m -ary modulation, the number of affected symbols in each switch in a subsequent round is at most $(m + 2)$. Therefore, in the subsequent rounds of the simplified BSA, we calculate the cost function only for the symbols that are affected by the most recent switch. This modification makes the BSA much simpler while resulting in the exactly same results.

V. NUMERICAL RESULTS AND DISCUSSION

This section provides resulting mappings and selected numerical results to illustrate the performance and advantage of our proposed MD mappings for BICM-ID.

A. Resulting MD Mappings

Our proposed algorithm is used to obtain MD mappings of different modulations such as 8-PSK, the optimum 8-QAM [27], and 2^m -QAM for $m = 4, 5, \dots, 10$. Tables I-II show the resulting 2-D mappings, i.e., λ_{er} , λ_{or} , λ_{el} , and λ_{ol} , in decimal format for 8-ary modulations and 16-QAM.

TABLE I
PROPOSED λ_{er} , λ_{or} , λ_{el} , AND λ_{ol} FOR 8-ARY MODULATIONS.

	8-PSK							Optimum 8-QAM								
λ_{er}	[2	7	6	5	4	1	0	3]	[1	3	5	7	2	0	6	4]
λ_{or}	[4	1	0	3	2	7	6	5]	[6	4	2	0	5	7	1	3]
λ_{el}	[(2,	6)	(1,	5)	(0,	4)	(3,	7)]	[(1,	5)	(3,	7)	(2,	6)	(0,	4)]
λ_{ol}	[(1,	5)	(0,	4)	(3,	7)	(2,	6)]	[(2,	6)	(3,	7)	(0,	4)	(1,	5)]

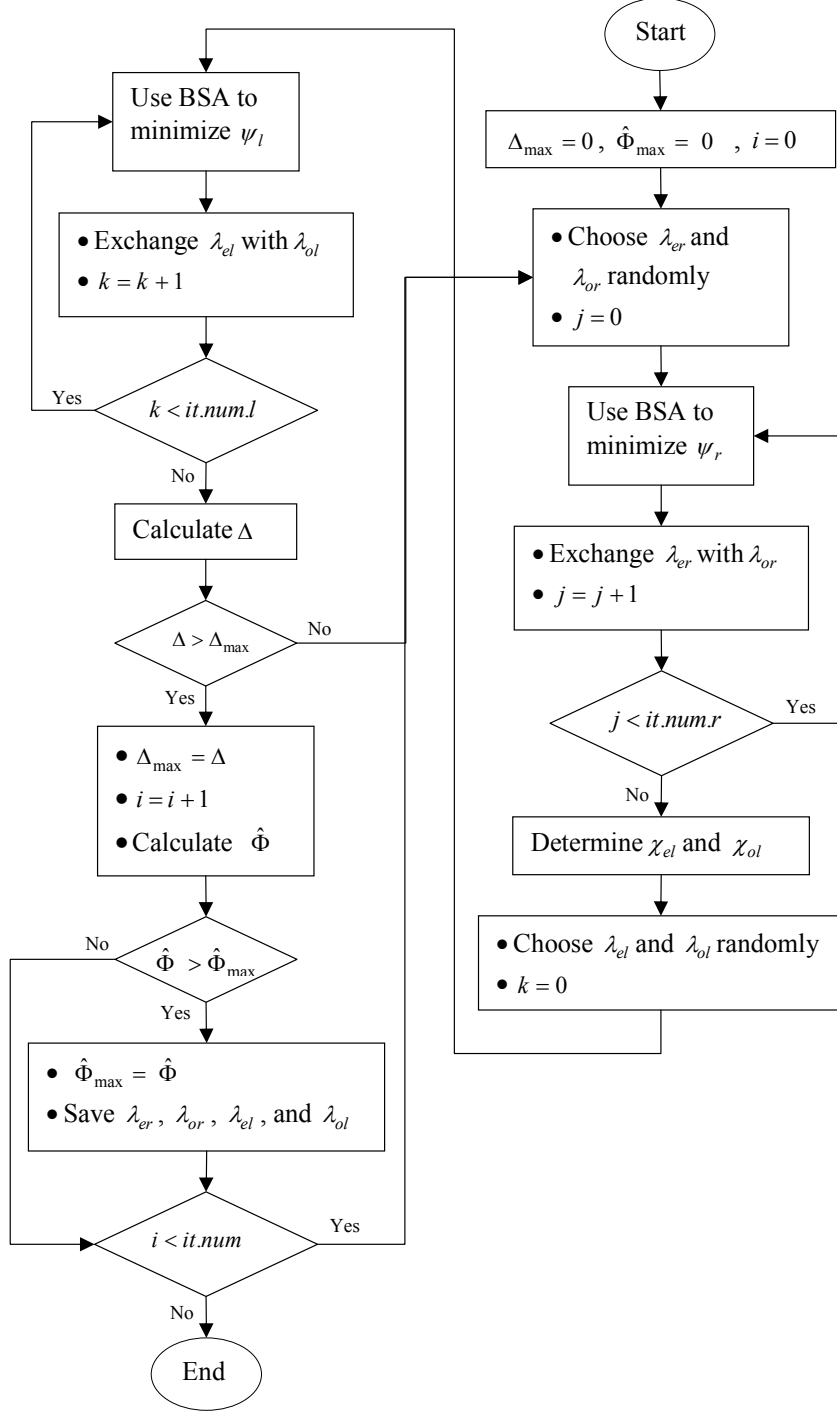


Fig. 2. Flowchart of the proposed algorithm ($it.num.r$, $it.num.l$, and $it.num$ represent the number of iterations for different loops).

The results for larger modulations are reported in Appendix E. In these tables, the decimal labels are ordered according to the symbol order in the corresponding constellations. For 8-PSK and the optimum 8-QAM, the considered symbol order is shown in Fig. 3. For square QAMs, it is assumed that the symbol order starts from the top left corner in the constellation and increases from top to bottom and from left to right (see Fig. 4.(a) as an example for 16-QAM). For cross QAM

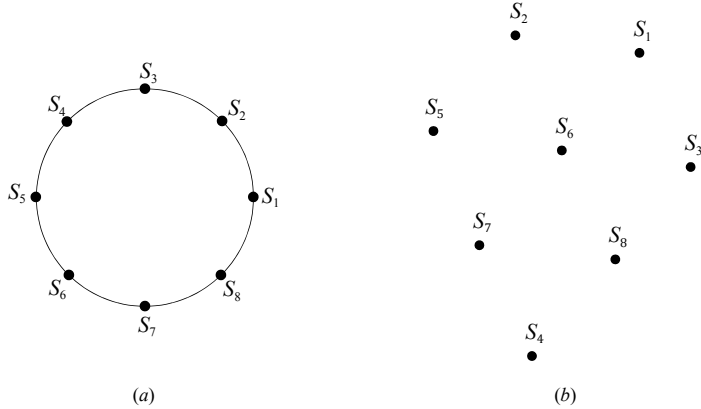


Fig. 3. (a). Symbol's arrangement in 8-ary constellations: (a). 8-PSK and (b). the optimum 8-QAM [27].

S_1	S_5	S_9	S_{13}	3	7	0	1	12	13	10	14	3,11	7,15	0,8	1,9
S_2	S_6	S_{10}	S_{14}	2	6	4	5	8	9	11	15	2,10	6,14	4,12	5,13
S_3	S_7	S_{11}	S_{15}	15	14	12	8	5	1	3	2	5,13	1,9	3,11	2,10
S_4	S_8	S_{12}	S_{16}	11	10	13	9	4	0	7	6	4,12	0,8	7,15	6,14

Fig. 4. (a). Symbol's arrangement in 16-QAM, and achieved 16-QAM mappings in decimal format: (b). λ_{er} , (c). λ_{or} , and (d). λ_{el} (the unshaded symbols), λ_{ol} (the shaded symbols).

constellations, such as 32-QAM, we consider the symbol order used in [28]. In these tables, the resulting 2-D mappings for higher order modulations are indicated in multiple rows. For example in Table VII, λ_{er} for 64-QAM is indicated in two rows, where the first element in the second row is the label of the 33rd symbol in the 64-QAM constellation. In addition, two labels in the i^{th} parentheses in λ_{el} and λ_{ol} in each table belong to the i^{th} symbol in χ_{el} and χ_{ol} , respectively. For example, Fig. 4.(b), (c), and (d) illustrate the 16-QAM mappings reported in Table II. As mentioned in Section IV-B, χ_{el} involves the symbols whose binary labels in λ_{er} take the value zero at the first bit position. In other words, χ_{el} is constructed by the symbols whose decimal label in λ_{er} is smaller than $\frac{M}{2}$. As a result, for 16-QAM, $\chi_{el} = \{S_1, S_2, S_5, S_6, S_9, S_{10}, S_{13}, S_{14}\}$, where χ_{el} is indicated by unshaded symbols in Fig. 4.(d). The remaining 16-QAM symbols belong to χ_{ol} , which are shaded in Fig. 4.(d). Example 1 clarifies how to use λ_{el} , λ_{ol} , λ_{er} , and λ_{or} to construct the proposed MD mapping of 16-QAM.

Example 1. In the proposed MD mapping method, let us set $m = 4$ (16-QAM), $N = 3$ and

TABLE II
PROPOSED λ_{er} , λ_{or} , λ_{el} , AND λ_{ol} FOR 16-QAM.

λ_{er}	[3 2 15 11 7 6 14 10 0 4 12 13 1 5 8 9]
λ_{or}	[12 8 5 4 13 9 1 0 10 11 3 7 14 15 2 6]
λ_{el}	[(3, 11) (2, 10) (7, 15) (6, 14) (0, 8) (4, 12) (1, 9) (5, 13)]
λ_{ol}	[(5, 13) (4, 12) (1, 9) (0, 8) (3, 11) (7, 15) (2, 10) (6, 14)]

$\mathbf{l} = (0, 1, 1, 0, 1, 1, 1, 0, 1, 1, 1)$. The label \mathbf{l} is considered as a sequence of three 4-bit labels, i.e., $\mathbf{l} = (\mathbf{l}_1, \mathbf{l}_2, \mathbf{l}_3)$, where $\mathbf{l}_1 = (0, 1, 1, 0)$, $\mathbf{l}_2 = (1, 1, 1, 1)$, and $\mathbf{l}_3 = (0, 1, 1, 1)$. The mapping rule in (6) is used to map $\mathbf{l} = (\mathbf{l}_1, \mathbf{l}_2, \mathbf{l}_3)$ to signal point $\mathbf{x} = (x_1, x_2, x_3)$, as follows. The Hamming weight of \mathbf{l} is odd, i.e., $\mathbf{l} \in \mathcal{L}_o$, thus $x_1 = \lambda_{ol}(\mathbf{l}_1)$, $x_2 = \lambda_{or}(\mathbf{l}_2)$, and $x_3 = \lambda_{or}(\mathbf{l}_3)$. The decimal format of \mathbf{l}_1 , \mathbf{l}_2 , and \mathbf{l}_3 are 6, 15, and 7, respectively. In Fig. 4(d), it can be observed that among the shaded symbols that λ_{ol} operates on, symbol S_{16} is mapped by decimal label 6. As a result, $x_1 = S_{16}$. Considering the mapping function λ_{or} indicated in Fig. 4(c) we also have $x_2 = \lambda_{or}(15) = S_{14}$ and $x_3 = \lambda_{or}(7) = S_{12}$. Consequently, \mathbf{l} is mapped to $\mathbf{x} = (S_{16}, S_{14}, S_{12})$.

B. Performance Comparison

The proposed mappings are compared to the MD mappings obtained using the state of the art methods in the literature such as the optimum mapping method in [11], the BSA, random mapping, and the MD mapping method in [12]. To assess different mappings, we first compare the value of $\Phi(\mu, \chi)$ and $\hat{\Phi}(\mu, \chi)$ offered by the mappings. Then, we use the BER curve to compare the BICM-ID error performance in the low SNR region when using different mappings. Finally, we use an analytical bound on the error-floor to evaluate the system's error performance in the high SNR region. In our simulations, we consider a rate-1/2 convolutional code with the generator polynomial of $(13, 15)_8$. An interleaver length of about 10000 bits is used. All BER curves are presented with seven iterations and all gains reported in this section are measured at a BER of 10^{-6} . Also, the error-floor bounds have been plotted using the Gauss-Chebyshev method in [22]. It is worth noting that achieving these error-floor bounds can be challenging because they happen at a very small value of BER.

TABLE III
COMPARISON OF $\Phi(\mu, \chi)$ AND $\hat{\Phi}(\mu, \chi)$ FOR DIFFERENT MAPPINGS.

Mapping	$N = 2$		$N = 3$	
	$\Phi(\mu, \chi)$	$\hat{\Phi}(\mu, \chi)$	$\Phi(\mu, \chi)$	$\hat{\Phi}(\mu, \chi)$
Optimum MD 8-PSK [11]	0.3112	3.3529	0.2119	3.5454
Proposed MD 8-PSK	0.3112	3.3529	0.2119	3.5454
BSA MD optimum 8-QAM	0.4506	2.7838	0.3002	2.8515
Proposed MD optimum 8-QAM	0.4552	2.9697	0.3041	3.1463

According to the modulation order, we discuss our results for three classes of modulations: low, medium, and high order modulations. In particular, we discuss 8-ary modulations (for the low order), 16- and 32-QAM (for the medium order), and M-QAM ($M = 64, 128$ and 256) for the higher order modulations.

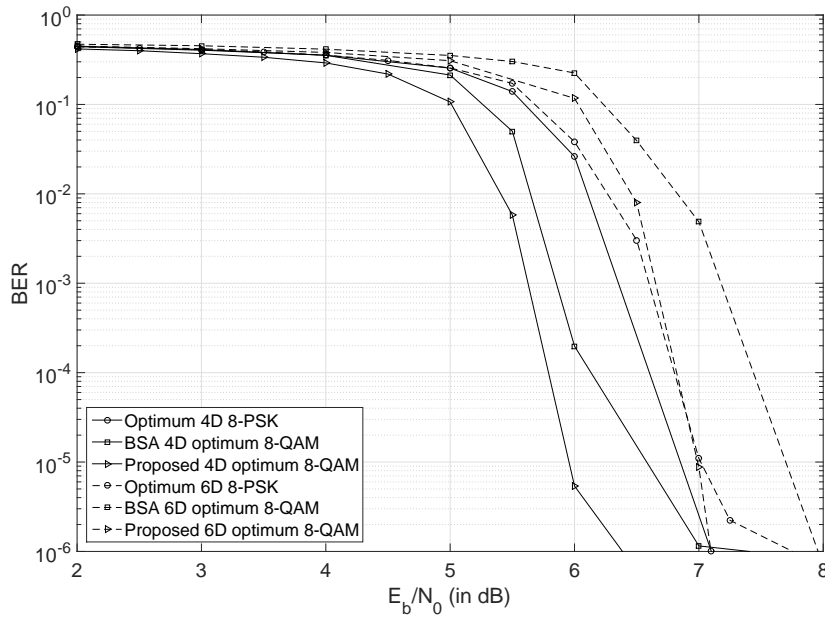


Fig. 5. BER performance of BICM-ID with 4-D and 6-D 8-ary modulations over Rayleigh fading channels.

1) *MD mapping of low order modulations:* Table III compares the values of the harmonic mean before and after feedback, i.e., $\Phi(\mu, \chi)$ and $\hat{\Phi}(\mu, \chi)$, for different $2N$ -D ($N = 2, 3$) mappings of 8-ary modulations. As this table shows, for 8-PSK, our proposed MD mapping provides the same values as those of the optimum MD mapping proposed in [11]. This clearly shows our proposed algorithm's efficiency. We have also used our algorithm to obtain MD mappings of the optimum 8-QAM constellation introduced in [27]. As shown in Table III, for the optimum 8-QAM, our resulting

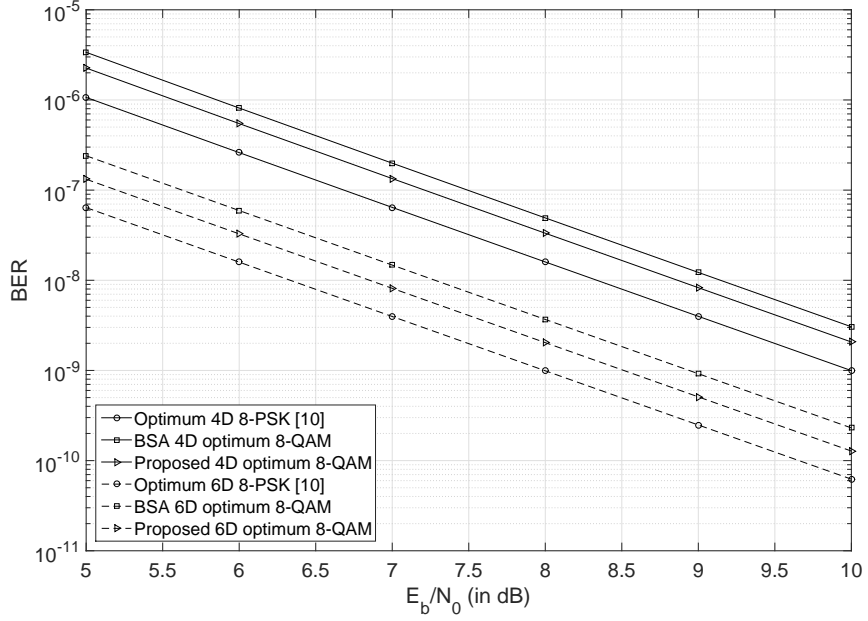


Fig. 6. Error-floor bounds of BER for BICM-ID with 4-D and 6-D 8-ary modulations over Rayleigh fading channels.

mappings improve the values of $\Phi(\mu, \chi)$ and $\hat{\Phi}(\mu, \chi)$ in comparison with the mappings obtained using the state of the art BSA. Therefore, it is expected that for the optimum 8-QAM, the proposed mappings outperform the BSA mappings in both the low and high SNR regions. This is confirmed by the plotted simulation results for the BER and error-floor bounds of BICM-ID in Fig. 5 and Fig. 6, respectively. As shown in Fig. 5, for the 4-D and 6-D optimum 8-QAM, our proposed mappings outperform their BSA counterparts by 1 and 0.85 dB, respectively. The gain over the optimum 4-D and 6-D mapping of 8-PSK is 0.7 and 0.65, respectively. This is because in addition to a large value of $\hat{\Phi}(\mu, \chi)$, the proposed MD mapping of the optimum 8-QAM significantly improves the value of $\Phi(\mu, \chi)$ compared to that of the optimum MD 8-PSK. Note that for the case of MD 8-PSK, our resulting mapping is the same as the optimum mapping in [11]. Thus, only the optimum mapping is used for comparison in BER and error-floor plots. As shown in Fig. 6, the proposed 4-D and 6-D mappings of the optimum 8-QAM outperform the corresponding BSA mappings by 0.3 and 0.45 dB, respectively. Moreover in this figure, the optimum MD mapping of 8-PSK offers a lower error-floor due to the nature of the 8-PSK constellation, which can offer higher values of $\hat{\Phi}(\mu, \chi)$.

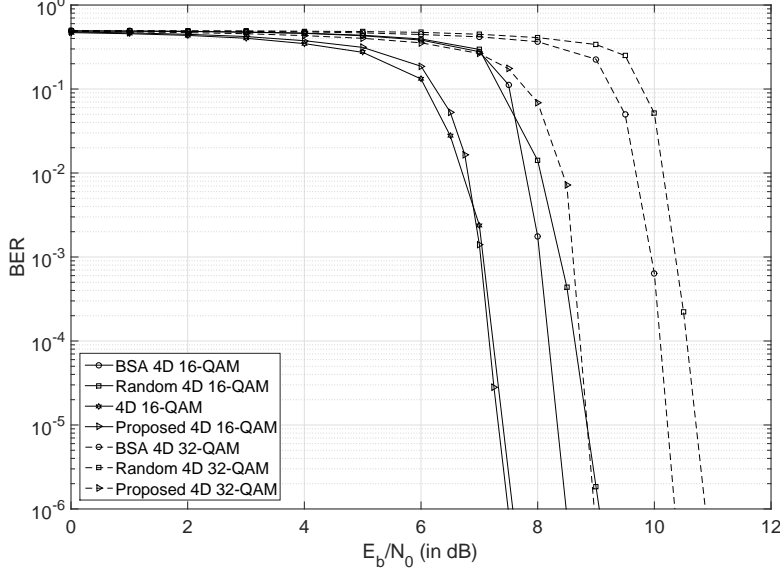


Fig. 7. BER performance of BICM-ID with 4-D 16- and 32-QAM over Rayleigh fading channels.

2) *MD mapping of medium order modulations:* Table IV lists the values of $\Phi(\mu, \chi)$ and $\hat{\Phi}(\mu, \chi)$ for different 4-D mappings of 16- and 32-QAM. It can be seen from this table that, except for the value of $\Phi(\mu, \chi)$ for the 4-D 16-QAM where the proposed mapping offers the same value as that of the mapping in [12], our proposed mappings significantly improve the values of $\Phi(\mu, \chi)$ and $\hat{\Phi}(\mu, \chi)$, compared to their well-known counterparts. Therefore, it is expected that the proposed mappings improve the error rate performance compared to the previously known mappings in both the low and high SNR regions. This is confirmed by the simulation results for the BER performance of BICM-ID shown in Fig. 7 and by the error-floor bounds plotted in Fig. 8. In the case of 4-D 16-QAM, as illustrated in Fig. 7, in the low SNR region, the proposed mapping achieves a gain

TABLE IV
COMPARISON OF $\Phi(\mu, \chi)$ AND $\hat{\Phi}(\mu, \chi)$ FOR DIFFERENT MAPPINGS.

4D Mapping		$\Phi(\mu, \chi)$	$\hat{\Phi}(\mu, \chi)$
16-QAM	BSA mapping	0.2026	2.5814
	Random mapping	0.2012	1.4350
	Mapping in [12]	0.2151	2.8491
	Proposed mapping	0.2151	3.1622
32-QAM	BSA mapping	0.1027	2.8574
	Random mapping	0.1008	1.2567
	Proposed mapping	0.1117	3.1677

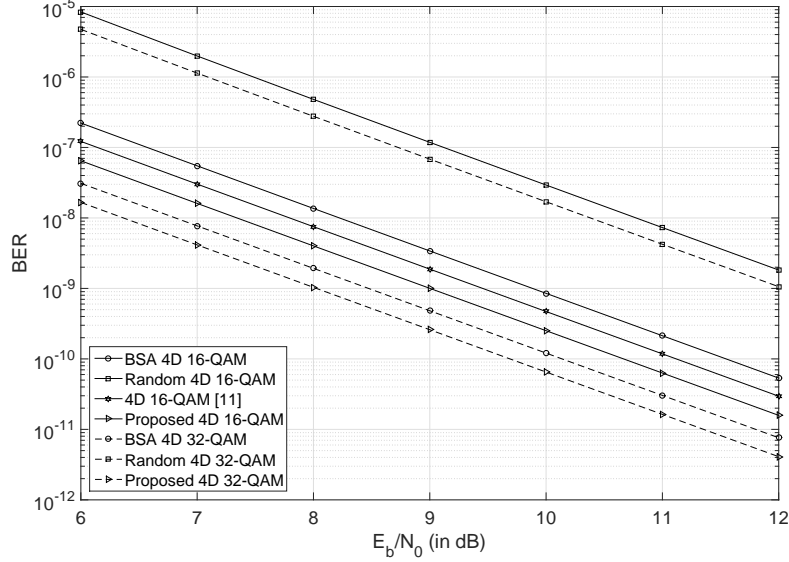


Fig. 8. Error-floor bounds of BER for BICM-ID with 4-D 16- and 32-QAM over Rayleigh fading channels.

of 1 and 1.55 dB over the BSA and random mappings, respectively. Although as shown in Fig. 7 the BER performance of the proposed 4-D 16-QAM is similar to that of the mapping in [12], our mapping outperforms the mapping in [12] in the high SNR region by about 0.5 dB, as shown in Fig. 8. This figure also shows that the proposed mapping improves the error-floor by 0.9 and 3.4 dB compared to the BSA and random mappings, respectively. In the case of 4-D 32-QAM, our proposed mapping outperforms the best previously known mappings, i.e., the BSA and random mappings, by 1.4 and 1.9 dB, respectively, which is illustrated in Fig. 7. Fig. 8 shows that the corresponding gain in the high SNR region is 0.5 and 4 dB, respectively.

3) *MD mapping of higher order modulations:* Table V reports the values of $\Phi(\mu, \chi)$ and $\hat{\Phi}(\mu, \chi)$ for MD mappings of different higher order modulations. It can be observed from this table that our proposed mappings improve these values compared to the previously known mappings, except for the case of the MD 64-QAM in [12], where our mapping offers a similar value of $\Phi(\mu, \chi)$. Therefore, it is expected that the proposed mappings offer improved error performance in both the low and high SNR regions. This is confirmed by the simulation results for the BER and by the analytical error bounds in Fig. 9-12. In the case of 4-D 64-QAM, our proposed mapping outperforms the BSA and random mappings in the low SNR region by 2.9 and 3.1 dB, respectively, as shown in Fig. 9.

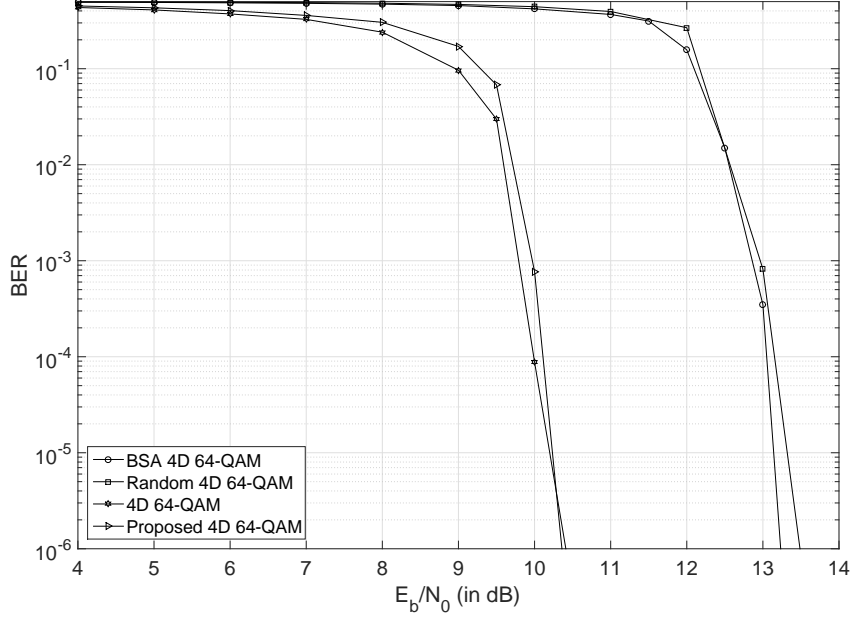


Fig. 9. BER performance of BICM-ID with 4-D 64-QAM over Rayleigh fading channels.

Although in Fig. 9 our proposed mapping offers similar performance to that of the mapping in [12], the proposed mapping outperforms the mapping in [12] by over 0.5 dB in the high SNR region, as shown in Fig. 10. In this figure, the achieved gain over the BSA and random mappings is 0.75 and 4.3 dB, respectively. As shown in Fig. 11, for 4-D 128-QAM in the low SNR region, the proposed mapping achieves the gain of 3.1 and 3 dB over the BSA and random mappings, respectively. The corresponding gain for the case of 4-D 256-QAM is 3.5 and 3.2 dB, respectively. For the case of 4-D 128-QAM in the high SNR region, our proposed mapping improves the error-floor by 2 and

TABLE V
COMPARISON OF $\Phi(\mu, \chi)$ AND $\hat{\Phi}(\mu, \chi)$ FOR DIFFERENT MAPPINGS.

4D Mapping		$\Phi(\mu, \chi)$	$\hat{\Phi}(\mu, \chi)$
64-QAM	BSA mapping	0.0481	2.6899
	Random mapping	0.0478	1.1688
	Mapping in [12]	0.0579	2.8166
	Proposed mapping	0.0568	3.1683
128-QAM	BSA mapping	0.0245	1.8566
	Random mapping	0.0245	1.1430
	Proposed mapping	0.0294	3.2273
256-QAM	BSA mapping	0.0118	1.1282
	Random mapping	0.0120	1.1034
	Proposed mapping	0.0144	3.2389

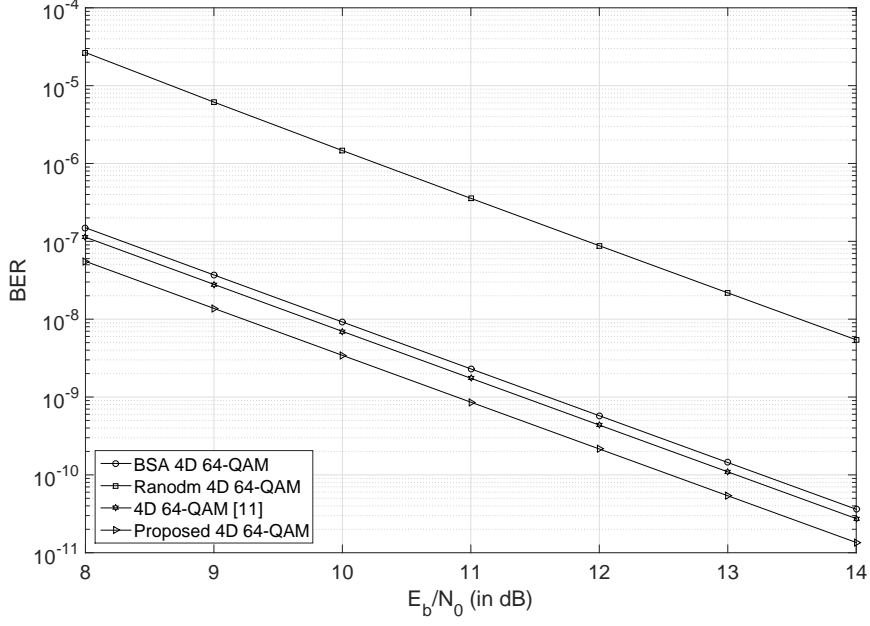


Fig. 10. Error-floor bounds of BER for BICM-ID with 4-D 64-QAM over Rayleigh fading channels.

4.5 dB compared to the BSA and random mappings, respectively, as illustrated in Fig. 12. The corresponding gain for the case of 4-D 256-QAM is 4.5 and 4.6 dB, respectively.

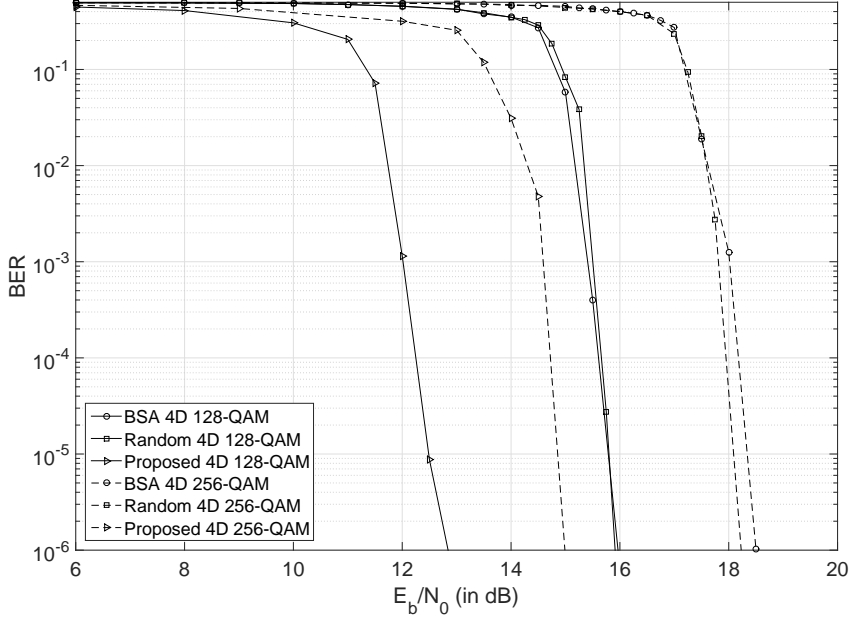


Fig. 11. BER performance of BICM-ID with 4-D 128- and 256-QAM over Rayleigh fading channels.

It can be observed from Fig. 5-12 that the BSA results become less efficient as the modulation

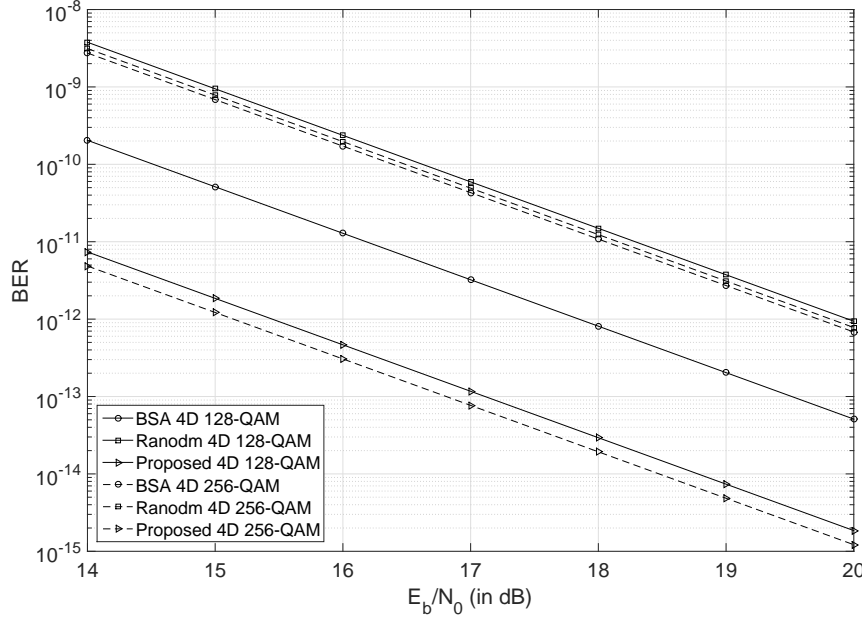


Fig. 12. Error-floor bounds of BER for BICM-ID with 4-D 128- and 256-QAM over Rayleigh fading channels.

order increases. As such, random mapping performs better than the BSA mapping for 4-D 256-QAM, as shown in Fig. 11.

Fig. 13 plots the BER curves for different MD mappings of 1024-QAM. As it can be seen from this figure, the proposed mapping significantly outperforms the other counterparts. It is also worth noting that in this figure, the random mapping outperforms the BSA mapping. This is because when looking for a mapping for 4-D 1024-QAM, the BSA is unable to finish one round of the algorithm in a reasonable time frame. As a result, the obtained BSA mapping is not very suitable.

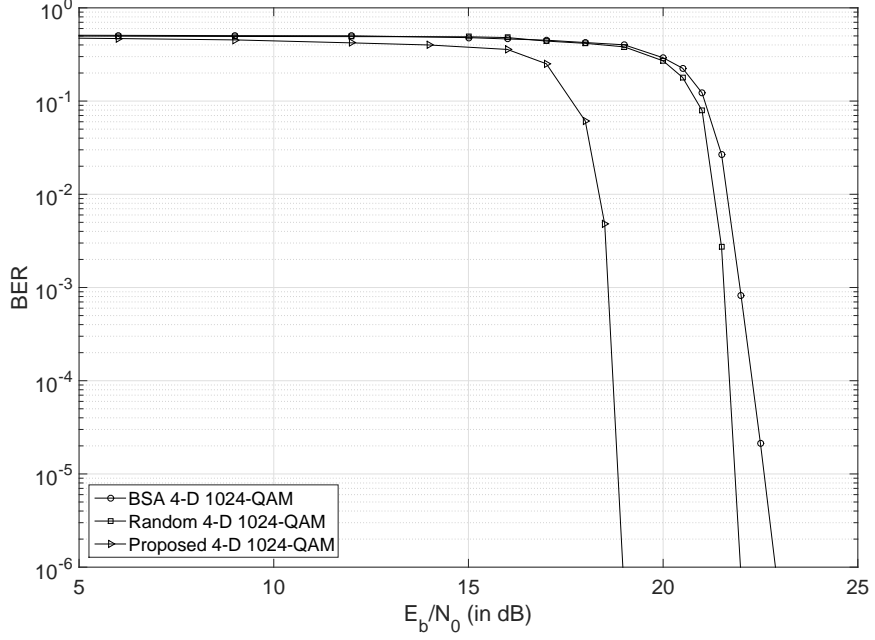


Fig. 13. BER performance of BICM-ID with 4-D 1024-QAM over Rayleigh fading channels.

C. Analysis of Convergence Behaviour

The extrinsic information transfer chart (EXIT chart) [17] is a commonly used metric to assess the convergence behavior of BICM-ID. In an EXIT chart, the area between the decoder curve and the demapper curve is called EXIT tunnel [16]. BICM-ID can achieve a coding gain through the iterative decoding process only when it provides an open EXIT tunnel. Fig. 14 shows the EXIT charts for BICM-ID when using different 4-D mappings of 128-QAM in the Rayleigh fading channel. For brevity in this section, we investigate the EXIT chart only for 4-D 128-QAM. The results are similar for other considered modulations. From Fig. 14, it can be seen that BICM-ID with the proposed mapping exhibits an open Exit tunnel when $\frac{E_b}{N_0} = 6$ dB. This implies that when using the proposed mapping, the iterative decoding process starts to improve the performance of BICM-ID at $\frac{E_b}{N_0} = 6$. This is in accordance with the BER curve of the proposed mapping in Fig. 11, where the BER curve falls gradually after $\frac{E_b}{N_0} = 6$. Fig. 14 also shows that the open EXIT tunnels for the BSA and random mappings appear at $\frac{E_b}{N_0} = 11$. As a result, when using the BSA and random mappings, the system BER will not improve unless after $\frac{E_b}{N_0} = 11$, which is confirmed by the corresponding BER curves in Fig. 11. Consequently, the BER performance with our proposed mapping improves through the

iterative decoding 5 dB earlier than those of the BSA and Random mappings. This results in an earlier turbo cliff for the BER curve with our proposed mapping in Fig. 11.

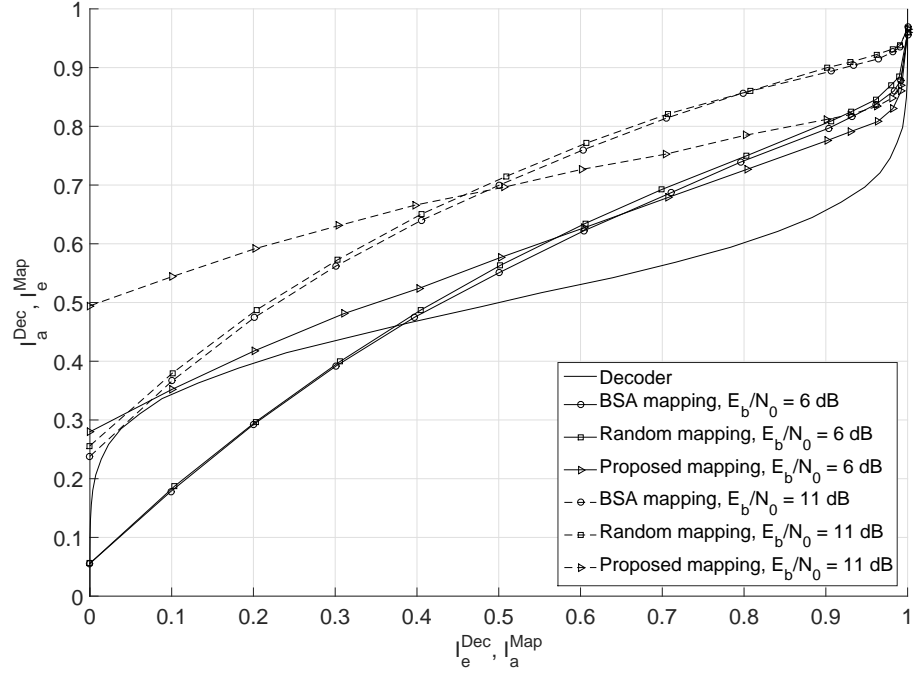


Fig. 14. EXIT chart for different 4-D mappings of 128-QAM in the Rayleigh fading channel.

VI. CONCLUSION

A novel MD mapping method is proposed to improve the error performance of the BICM-ID system in both the low and high SNR regions over Rayleigh fading channels. The method uses four 2-D mappings to construct an MD mapping that improves the error performance in the low SNR region. Furthermore, cost functions are developed and optimized over the 2-D mappings to achieve an MD mapping that improves the error performance in the high SNR region. Due to the lower complexity of the 2-D space, the optimization approach is very simple and results in excellent MD mappings for different modulations, including higher order modulations such as 2^m -QAM ($m = 4, \dots, 10$). Extensive numerical results, including analytical and simulation results, show that the obtained mappings significantly outperform the previously known state of the art mappings in both the low and high SNR regions.

APPENDIX A

PROOF OF PROPOSITION 1

Let $\mathbf{i} = (i_1, i_2, \dots, i_D)$ be the set of bit positions at which \mathbf{l}_1 and \mathbf{l}_2 are different. Let us define o_j and z_j as

$$\begin{aligned} o_j &= \sum_{k=1}^D I(l_j^{i_k} = 1), \\ z_j &= \sum_{k=1}^D I(l_j^{i_k} = 0), \end{aligned} \tag{29}$$

where $j = 1, 2$ and $I(\theta)$ is an indicator function that takes value one if θ is true, otherwise it equals zero. Clearly, $z_1 = o_2$ and $z_2 = o_1$. Let \bar{o} be the number of bit positions in which both \mathbf{l}_1 and \mathbf{l}_2 represent the bit value one. As $w_1 = o_1 + \bar{o}$ and $w_2 = o_2 + \bar{o}$, we can write

$$\begin{aligned} W = w_1 + w_2 &= (o_1 + \bar{o}) + (o_2 + \bar{o}), \\ &= o_1 + o_2 + 2\bar{o}, \\ &\stackrel{(o_2=z_1)}{=} o_1 + z_1 + 2\bar{o}, \\ &= D + 2\bar{o}. \end{aligned} \tag{30}$$

In (30), $2\bar{o}$ is an even number; as a result, if $W \in \mathbb{E}$, $D \in \mathbb{E}$, and if $W \in \mathbb{O}$, $D \in \mathbb{O}$.

APPENDIX B

PROOF OF PROPOSITION 2

Let \mathbf{l} and $\tilde{\mathbf{l}}$ be two mN -bit labels. If $\mathbf{l}, \tilde{\mathbf{l}} \in \mathcal{L}_e$ or $\mathbf{l}, \tilde{\mathbf{l}} \in \mathcal{L}_o$, the corresponding value for W in Proposition 1 is an even number. As a result, \mathbf{l} and $\tilde{\mathbf{l}}$ have an even Hamming distance from each other. Similarly, two labels one from \mathcal{L}_e and the other from \mathcal{L}_o have an odd Hamming distance from each other. Since there is no common 2-D signal point between χ_{el} and χ_{ol} , there is no common 2N-D signal point between χ_e and χ_o . As a result, none of the 2N-D signal points will be mapped simultaneously by a label from \mathcal{L}_e and a label from \mathcal{L}_o . Therefore, it is sufficient to prove that there

is a one-to-one correspondence between labels from \mathcal{L}_e and signal points from χ_e and similarly between labels in \mathcal{L}_o and signal points in χ_o . In what follows, we prove this for the even subsets, i.e., for labels in \mathcal{L}_e and signal points in χ_e .

Assume that $\mathbf{l} = (l_1, l_2, \dots, l_{mN})$ and $\tilde{\mathbf{l}} = (\tilde{l}_1, \tilde{l}_2, \dots, \tilde{l}_{mN})$ are two labels in \mathcal{L}_e and are mapped to $\mathbf{x} = (x_1, \dots, x_N)$ and $\tilde{\mathbf{x}} = (\tilde{x}_1, \dots, \tilde{x}_N)$, respectively, where both \mathbf{x} and $\tilde{\mathbf{x}}$ are in χ_e . Let us define \mathbf{l}_i and $\tilde{\mathbf{l}}_i$ as the i^{th} m -tuple bits of \mathbf{l} and $\tilde{\mathbf{l}}$, respectively. Then $\mathbf{l} = (l_1, l_2, \dots, l_N)$ and $\tilde{\mathbf{l}} = (\tilde{l}_1, \tilde{l}_2, \dots, \tilde{l}_N)$. Based on the relation between \mathbf{l}_i and $\tilde{\mathbf{l}}_i$ for different values of i , there are two possible cases as follows:

Case 1: There exists a value of i ($i \geq 2$) such that $l_i \neq \tilde{l}_i$. Let $j \geq 2$, then according to (6), the same one-to-one mapping function, i.e., $\lambda_{er}(.)$, is used to map \mathbf{l}_j to x_j and $\tilde{\mathbf{l}}_j$ to \tilde{x}_j . Therefore, because $l_j \neq \tilde{l}_j$, we have

$$x_j \neq \tilde{x}_j \Rightarrow \mathbf{x} \neq \tilde{\mathbf{x}}. \quad (31)$$

Case 2: $l_i = \tilde{l}_i$ for all $i \geq 2$. In this case, $l_i \neq \tilde{l}_i$ only when $i = 1$, and as a result, $d_H(\mathbf{l}, \tilde{\mathbf{l}}) = d_H(l_1, \tilde{l}_1)$. Since \mathbf{l} and $\tilde{\mathbf{l}}$ belong to \mathcal{L}_e , they have an even Hamming distance from each other. Consequently, the Hamming distance between l_1 and \tilde{l}_1 is even as well. However, the two labels that are mapped to each symbol in χ_{el} have an odd Hamming distance from each other. Therefore, because $\lambda_{el}(\mathbf{l}_1) \neq \lambda_{el}(\tilde{\mathbf{l}}_1)$, we have

$$x_1 \neq \tilde{x}_1 \Rightarrow \mathbf{x} \neq \tilde{\mathbf{x}}. \quad (32)$$

From (31) and (32), it is concluded that in the proposed mapping function, different labels from \mathcal{L}_e are mapped to different signal points in χ_e . In a similar way, it can be proven that the different labels from \mathcal{L}_o are mapped to the different signal points in χ_o . As a result, the proposed MD mapping function is bijective.

APPENDIX C

PROOF OF PROPOSITION 3

Similar to proposition 1, assume that $\mathbf{l} = (\mathbf{l}_1, \mathbf{l}_2, \dots, \mathbf{l}_N)$ and $\mathbf{l}' = (\mathbf{l}'_1, \mathbf{l}'_2, \dots, \mathbf{l}'_N)$ are two labels in \mathcal{L}_e and are mapped to $\mathbf{x} = (x_1, \dots, x_N)$ and $\mathbf{x}' = (x'_1, \dots, x'_N)$, respectively, where both \mathbf{x} and \mathbf{x}' are in χ_e , and \mathbf{l}_i and \mathbf{l}'_i are the i^{th} m -tuple bits of \mathbf{l} and \mathbf{l}' , respectively. Let us assume that $d_H(\mathbf{l}, \mathbf{l}') \geq m + 2$ and j is the number of values for i such that $\mathbf{l}_i \neq \mathbf{l}'_i$. Note that $d_H(\mathbf{l}, \mathbf{l}') > m$, thus $j > 1$. Based on the value of j , there are two possible cases as follows.

Case 1 (when $j = 2$): Assume that $\mathbf{l}_i \neq \mathbf{l}'_i$ for $i = p, q$, where $q > p \geq 1$. We have

$$d_H(\mathbf{l}, \mathbf{l}') = d_H(\mathbf{l}_p, \mathbf{l}'_p) + d_H(\mathbf{l}_q, \mathbf{l}'_q). \quad (33)$$

Let $p = 1$. Because \mathbf{l}_q and \mathbf{l}'_q are m -tuple vectors, $d_H(\mathbf{l}_q, \mathbf{l}'_q) \leq m$. Moreover, $d_H(\mathbf{l}, \mathbf{l}') \geq m + 2$. Thus, using (33) we have $d_H(\mathbf{l}_p, \mathbf{l}'_p) \geq 2$. Since $p = 1$, the mapping function λ_{el} in (6) is used to map \mathbf{l}_p and \mathbf{l}'_p . Note that in λ_{el} , two m -tuple labels with Hamming distance more than one bit cannot be mapped to the same 2-D symbol. As a result, we have $\lambda_{el}(\mathbf{l}_p) \neq \lambda_{el}(\mathbf{l}'_p)$, and therefore, $x_p \neq x'_p$. Similarly, since $q > 1$, the mapping function λ_{er} in (6) is used to map \mathbf{l}_q and \mathbf{l}'_q . Moreover, λ_{er} in (6) maps different m -tuple labels to different 2-D symbols. Therefore, as $\mathbf{l}_q \neq \mathbf{l}'_q$, $\lambda_{er}(\mathbf{l}_q) \neq \lambda_{er}(\mathbf{l}'_q)$, and as a result, $x_q \neq x'_q$. Let $p > 1$. In this case, λ_{er} is used to map \mathbf{l}_p , \mathbf{l}'_p , \mathbf{l}_q , and \mathbf{l}'_q . As $\mathbf{l}_p \neq \mathbf{l}'_p$ and $\mathbf{l}_q \neq \mathbf{l}'_q$, $\lambda_{er}(\mathbf{l}_p) \neq \lambda_{er}(\mathbf{l}'_p)$ and $\lambda_{er}(\mathbf{l}_q) \neq \lambda_{er}(\mathbf{l}'_q)$. As a result, $x_p \neq x'_p$ and $x_q \neq x'_q$. Therefore, for all values of p and q , \mathbf{x} and \mathbf{x}' are different in more than one symbol.

Case 2 (when $j \geq 3$): There are at least two values, p and q , such that $p > q > 1$ and $\mathbf{l}_i \neq \mathbf{l}'_i$ when $i = p, q$. In this case, λ_{er} is used to map \mathbf{l}_p , \mathbf{l}'_p , \mathbf{l}_q , and \mathbf{l}'_q . As $\mathbf{l}_p \neq \mathbf{l}'_p$ and $\mathbf{l}_q \neq \mathbf{l}'_q$, $\lambda_{er}(\mathbf{l}_p) \neq \lambda_{er}(\mathbf{l}'_p)$ and $\lambda_{er}(\mathbf{l}_q) \neq \lambda_{er}(\mathbf{l}'_q)$. As a result, $x_i \neq x'_i$ when $i = p, q$. Therefore, \mathbf{x} and \mathbf{x}' are different in more than one symbol.

Consequently, in the proposed MD mapping function, when the Hamming distance between two labels in \mathcal{L}_e is larger than $(m + 1)$ bits, the corresponding symbols-vectors in χ_e are different in more than one symbol, and therefore, cannot be the nearest neighbours. The same characteristic can

TABLE VI
PROPOSED λ_{er} , λ_{or} , λ_{el} , AND λ_{ol} FOR 32-QAM.

λ_{er}	[24 17 13 8 25 29 1 9 21 28 0 5 16 20 4 12, 30 22 6 2 23 18 14 7 26 19 15 11 27 31 3 10]
λ_{or}	[7 2 30 22 6 14 18 23 10 15 19 26 3 11 27 31, 13 9 25 24 8 1 29 21 4 0 28 20 5 12 17 16]
λ_{el}	[(13 29) (8 24) (1 17) (9 25) (0 16) (5 21) (4 20) (12 28), (6 22) (2 18) (14 30) (7 23) (15 31) (11 27) (3 19) (10 26)]
λ_{ol}	[(7 23) (2 18) (6 22) (14 30) (10 26) (15 31) (3 19) (11 27), (13 29), (9 25) (8 24) (1 17) (4 20) (0 16) (5 21) (12 28)]

be proven for the labels in \mathcal{L}_o and the corresponding symbol-vectors in χ_o .

APPENDIX D

PROOF OF PROPOSITION 4

Since $y_i \geq 0$ for all i , then

$$\frac{1}{\sum_{i=1}^N y_i} \leq \frac{1}{y_j}, \quad j = 1, 2, \dots, N. \quad (34)$$

By taking the summation over all values of j from both sides of (34), the inequality in (12) can be written as

$$\frac{1}{\sum_{i=1}^N y_i} \leq \frac{1}{N} \sum_{j=1}^N \frac{1}{y_j}. \quad (35)$$

APPENDIX E

PROPOSED MAPPINGS

TABLE VII
PROPOSED λ_{er} , λ_{or} , λ_{el} , AND λ_{ol} FOR 64-QAM.

λ_{er}	[63 55 61 53 48 56 50 58 62 54 46 38 35 43 51 59, 60 52 36 37 32 33 49 57 47 39 44 45 40 41 34 42, 21 6 4 5 0 1 3 16 14 29 12 13 8 9 24 11, 22 30 28 20 17 25 27 19 23 31 15 7 2 10 26 18]
λ_{or}	[0 8 17 2 7 20 13 5 1 9 25 10 15 28 12 4, 16 24 27 26 31 30 29 21 3 11 19 18 23 22 14 6, 49 57 59 58 63 62 60 52 34 42 51 50 55 54 47 39, 41 33 56 48 53 61 36 44 40 32 43 35 38 46 37 45]
λ_{el}	[(14 46) (6 38) (4 36) (5 37) (0 32) (1 33) (3 35) (11 43), (30 62) (21 53) (12 44) (13 45) (8 40) (9 41) (16 48) (27 59), (22 54) (29 61) (20 52) (7 39) (2 34) (17 49) (24 56) (19 51), (23 55) (31 63) (28 60) (15 47) (10 42) (25 57) (26 58) (18 50)]
λ_{ol}	[(0 32) (8 40) (17 49) (2 34) (7 39) (20 52) (13 45) (5 37), (1 33) (16 48) (25 57) (10 42) (15 47) (28 60) (21 53) (4 36), (9 41) (24 56) (27 59) (26 58) (31 63) (22 54) (29 61) (12 44), (3 35) (11 43) (19 51) (18 50) (23 55) (30 62) (14 46) (6 38)]

TABLE VIII
PROPOSED λ_{er} , λ_{or} , λ_{el} , AND λ_{ol} FOR 128-QAM.

λ_{er}	[100 103 37 86 105 122 32 115 116 118 36 70 104 107 106 113, 102 110 126 111 127 96 114 98 119 101 108 124 109 82 66 99, 117 94 78 125 64 67 112 97 87 76 79 95 80 72 83 74, 68 71 92 77 88 65 75 90 61 84 69 93 73 89 91 120, 60 31 13 85 24 8 81 121 14 15 12 29 25 11 16 3, 30 5 21 28 9 27 17 19 52 23 7 20 57 56 26 1, 39 4 22 59 43 10 49 51 38 54 6 41 58 40 42 33, 53 46 47 63 18 2 50 48 62 55 44 45 0 123 34 35]
λ_{or}	[17 24 121 0 44 61 85 15 16 8 81 3 60 31 13 14, 25 9 27 56 20 21 28 29 11 26 40 59 57 4 5 12, 1 10 49 43 41 22 7 30 19 48 58 42 6 52 53 23, 18 35 51 33 54 39 55 47 123 2 50 34 38 46 62 37, 107 122 32 98 102 118 36 63 104 106 115 114 126 119 70 86, 113 97 99 96 110 100 103 116 83 112 82 66 111 101 78 117, 72 67 64 109 127 108 94 76 65 88 80 125 124 95 79 77, 74 89 90 120 68 71 69 87 75 73 91 105 45 84 93 92]
λ_{el}	[(37 101) (32 96) (36 100) (61 125) (60 124) (31 95) (13 77) (24 88), (8 72) (14 78) (15 79) (12 76) (29 93) (25 89) (11 75) (16 80), (3 67) (30 94) (5 69) (21 85) (28 92) (9 73) (27 91) (17 81), (19 83) (52 116) (23 87) (7 71) (20 84) (57 121) (56 120) (26 90), (1 65) (39 103) (4 68) (22 86) (59 123) (43 107) (10 74) (49 113), (51 115) (38 102) (54 118) (6 70) (41 105) (58 122) (40 104) (42 106), (33 97) (53 117) (46 110) (47 111) (63 127) (18 82) (2 66) (50 114), (48 112) (62 126) (55 119) (44 108) (45 109) (0 64) (34 98) (35 99)]
λ_{ol}	[(17 81) (24 88) (0 64) (45 109) (60 124) (15 79) (16 80) (8 72), (3 67) (63 127) (31 95) (13 77) (14 78) (25 89) (11 75) (9 73), (27 91) (57 121) (21 85) (28 92) (29 93) (56 120) (10 74) (40 104), (59 123) (20 84) (4 68) (7 71) (12 76) (26 90) (1 65) (49 113), (43 107) (41 105) (22 86) (23 87) (5 69) (19 83) (48 112) (51 115), (58 122) (6 70) (39 103) (52 116) (30 94) (18 82) (50 114) (35 99), (42 106) (54 118) (55 119) (62 126) (53 117) (2 66) (34 98) (33 97), (38 102) (46 110) (37 101) (47 111) (32 96) (36 100) (44 108) (61 125)]

TABLE IX
PROPOSED λ_{er} , λ_{or} , λ_{el} , AND λ_{ol} FOR 256-QAM.

λ_{er}	[206 205 222 237 236 220 252 211 227 195 194 135 215 204 231 199, 207 254 221 141 253 200 140 243 167 226 151 210 247 83 230 198, 238 142 201 88 217 157 216 156 131 209 242 166 193 134 213 197, 239 255 89 158 173 232 172 188 163 130 183 225 208 150 246 214, 223 218 174 233 249 189 248 136 162 147 241 129 165 81 245 229, 202 219 159 191 190 137 153 152 179 145 146 182 224 149 192 133, 203 234 250 138 154 169 185 168 177 161 240 144 181 80 244 212, 143 175 251 170 155 187 186 184 178 176 160 128 164 148 132 228, 91 235 139 60 171 25 24 56 49 17 51 180 35 3 115 99, 92 124 44 28 120 40 57 59 48 16 50 34 19 2 39 67, 12 72 29 61 121 8 41 58 32 33 113 18 55 114 98 7, 108 125 73 104 62 9 27 26 52 112 1 54 97 38 23 66, 93 109 13 45 105 63 10 42 43 0 53 96 22 65 82 103, 77 94 90 30 46 122 123 11 36 20 37 21 5 6 119 196, 76 95 126 14 127 31 106 47 116 4 117 64 118 102 85 71, 78 79 110 111 74 75 15 107 84 101 100 68 69 86 70 87]
	[49 48 16 32 112 0 52 36 43 42 27 26 58 59 57 56, 17 33 1 53 21 117 20 116 47 11 123 10 63 41 40 24, 50 113 54 96 37 64 84 4 107 106 46 122 105 62 9 25, 51 18 97 65 22 5 101 100 15 127 31 90 30 104 121 8, 34 55 114 38 6 118 69 68 75 74 14 13 73 45 61 120, 19 2 23 82 119 102 86 111 110 95 126 109 125 72 29 60, 35 3 98 7 66 103 85 70 79 77 94 108 12 124 44 28, 180 115 39 99 67 196 71 87 78 76 93 92 91 235 139 171, 80 148 244 228 212 229 197 198 206 207 239 203 143 234 175 170, 164 149 132 133 246 214 231 199 205 238 223 142 202 219 251 138, 128 224 192 245 213 230 215 204 222 237 221 255 218 159 250 155, 181 81 150 193 134 210 247 135 220 236 254 141 174 89 191 154, 240 165 225 208 151 83 194 195 211 200 253 201 158 233 249 187, 160 144 129 183 166 209 226 227 252 140 217 173 88 190 137 169, 176 161 182 241 130 242 167 131 243 216 157 232 189 153 185 186, 178 177 179 146 145 162 147 163 156 188 172 248 136 152 168 184]
λ_{or}	[1(83 211) (88 216) (89 217) (81 209) (80 208) (91 219) (60 188) (25 153), (24 152) (56 184) (49 177) (17 145) (51 179) (35 163) (3 131) (115 243), (99 227) (92 220) (124 252) (44 172) (28 156) (120 248) (40 168) (57 185), (59 187) (48 176) (16 144) (50 178) (34 162) (19 147) (2 130) (39 167), (67 195) (12 140) (72 200) (29 157) (61 189) (121 249) (8 136) (41 169), (58 186) (32 160) (33 161) (113 241) (18 146) (55 183) (114 242) (98 226), (7 135) (108 236) (125 253) (73 201) (104 232) (62 190) (9 137) (27 155), (26 154) (52 180) (112 240) (1 129) (54 182) (97 225) (38 166) (23 151), (66 194) (93 221) (109 237) (13 141) (45 173) (105 233) (63 191) (10 138), (42 170) (43 171) (0 128) (53 181) (96 224) (22 150) (65 193) (82 210), (103 231) (77 205) (94 222) (90 218) (30 158) (46 174) (122 250) (123 251), (11 139) (36 164) (20 148) (37 165) (21 149) (5 133) (6 134) (119 247), (76 204) (95 223) (126 254) (14 142) (127 255) (31 159) (106 234) (47 175), (116 244) (4 132) (117 245) (64 192) (118 246) (102 230) (85 213) (71 199), (78 206) (79 207) (110 238) (111 239) (74 202) (75 203) (15 143) (107 235), (84 212) (101 229) (100 228) (68 196) (69 197) (86 214) (70 198) (87 215)]
	[1(49 177) (48 176) (32 160) (112 240) (0 128) (53 181) (43 171) (52 180), (11 139) (10 138) (42 170) (26 154) (27 155) (58 186) (59 187) (56 184), (17 145) (33 161) (1 129) (54 182) (96 224) (21 149) (20 148) (36 164), (116 244) (122 250) (123 251) (63 191) (9 137) (41 169) (57 185) (16 144), (113 241) (97 225) (37 165) (117 245) (84 212) (4 132) (47 175) (31 159), (46 174) (30 158) (105 233) (62 190) (8 136) (24 152) (50 178) (18 146), (22 150) (5 133) (64 192) (101 229) (107 235) (106 234) (75 203) (127 255), (13 141) (45 173) (104 232) (121 249) (25 153) (51 179) (55 183) (38 166), (65 193) (6 134) (118 246) (68 196) (100 228) (15 143) (74 202) (14 142), (90 218) (73 201) (61 189) (40 168) (34 162) (2 130) (114 242) (23 151), (119 247) (102 230) (86 214) (69 197) (111 239) (110 238) (126 254) (109 237), (125 253) (72 200) (29 157) (120 248) (19 147) (115 243) (98 226) (82 210), (66 194) (103 231) (85 213) (70 198) (79 207) (95 223) (77 205) (94 222), (12 140) (44 172) (28 156) (35 163) (3 131) (39 167) (99 227) (7 135), (83 211) (71 199) (87 215) (78 206) (76 204) (93 221) (108 236) (92 220), (91 219) (124 252) (60 188) (80 208) (81 209) (67 195) (89 217) (88 216)]
λ_{el}	[1(83 211) (88 216) (89 217) (81 209) (80 208) (91 219) (60 188) (25 153), (24 152) (56 184) (49 177) (17 145) (51 179) (35 163) (3 131) (115 243), (99 227) (92 220) (124 252) (44 172) (28 156) (120 248) (40 168) (57 185), (59 187) (48 176) (16 144) (50 178) (34 162) (19 147) (2 130) (39 167), (67 195) (12 140) (72 200) (29 157) (61 189) (121 249) (8 136) (41 169), (58 186) (32 160) (33 161) (113 241) (18 146) (55 183) (114 242) (98 226), (7 135) (108 236) (125 253) (73 201) (104 232) (62 190) (9 137) (27 155), (26 154) (52 180) (112 240) (1 129) (54 182) (97 225) (38 166) (23 151), (66 194) (93 221) (109 237) (13 141) (45 173) (105 233) (63 191) (10 138), (42 170) (43 171) (0 128) (53 181) (96 224) (22 150) (65 193) (82 210), (103 231) (77 205) (94 222) (90 218) (30 158) (46 174) (122 250) (123 251), (11 139) (36 164) (20 148) (37 165) (21 149) (5 133) (6 134) (119 247), (76 204) (95 223) (126 254) (14 142) (127 255) (31 159) (106 234) (47 175), (116 244) (4 132) (117 245) (64 192) (118 246) (102 230) (85 213) (71 199), (78 206) (79 207) (110 238) (111 239) (74 202) (75 203) (15 143) (107 235), (84 212) (101 229) (100 228) (68 196) (69 197) (86 214) (70 198) (87 215)]
	[1(49 177) (48 176) (32 160) (112 240) (0 128) (53 181) (43 171) (52 180), (11 139) (10 138) (42 170) (26 154) (27 155) (58 186) (59 187) (56 184), (17 145) (33 161) (1 129) (54 182) (96 224) (21 149) (20 148) (36 164), (116 244) (122 250) (123 251) (63 191) (9 137) (41 169) (57 185) (16 144), (113 241) (97 225) (37 165) (117 245) (84 212) (4 132) (47 175) (31 159), (46 174) (30 158) (105 233) (62 190) (8 136) (24 152) (50 178) (18 146), (22 150) (5 133) (64 192) (101 229) (107 235) (106 234) (75 203) (127 255), (13 141) (45 173) (104 232) (121 249) (25 153) (51 179) (55 183) (38 166), (65 193) (6 134) (118 246) (68 196) (100 228) (15 143) (74 202) (14 142), (90 218) (73 201) (61 189) (40 168) (34 162) (2 130) (114 242) (23 151), (119 247) (102 230) (86 214) (69 197) (111 239) (110 238) (126 254) (109 237), (125 253) (72 200) (29 157) (120 248) (19 147) (115 243) (98 226) (82 210), (66 194) (103 231) (85 213) (70 198) (79 207) (95 223) (77 205) (94 222), (12 140) (44 172) (28 156) (35 163) (3 131) (39 167) (99 227) (7 135), (83 211) (71 199) (87 215) (78 206) (76 204) (93 221) (108 236) (92 220), (91 219) (124 252) (60 188) (80 208) (81 209) (67 195) (89 217) (88 216)]
λ_{ol}	[1(49 177) (48 176) (32 160) (112 240) (0 128) (53 181) (43 171) (52 180), (11 139) (10 138) (42 170) (26 154) (27 155) (58 186) (59 187) (56 184), (17 145) (33 161) (1 129) (54 182) (96 224) (21 149) (20 148) (36 164), (116 244) (122 250) (123 251) (63 191) (9 137) (41 169) (57 185) (16 144), (113 241) (97 225) (37 165) (117 245) (84 212) (4 132) (47 175) (31 159), (46 174) (30 158) (105 233) (62 190) (8 136) (24 152) (50 178) (18 146), (22 150) (5 133) (64 192) (101 229) (107 235) (106 234) (75 203) (127 255), (13 141) (45 173) (104 232) (121 249) (25 153) (51 179) (55 183) (38 166), (65 193) (6 134) (118 246) (68 196) (100 228) (15 143) (74 202) (14 142), (90 218) (73 201) (61 189) (40 168) (34 162) (2 130) (114 242) (23 151), (119 247) (102 230) (86 214) (69 197) (111 239) (110 238) (126 254) (109 237), (125 253) (72 200) (29 157) (120 248) (19 147) (115 243) (98 226) (82 210), (66 194) (103 231) (85 213) (70 198) (79 207) (95 223) (77 205) (94 222), (12 140) (44 172) (28 156) (35 163) (3 131) (39 167) (99 227) (7 135), (83 211) (71 199) (87 215) (78 206) (76 204) (93 221) (108 236) (92 220), (91 219) (124 252) (60 188) (80 208) (81 209) (67 195) (89 217) (88 216)]

TABLE X
PROPOSED λ_{er} AND λ_{or} FOR 512-QAM.

λ_{er}	[397 493 479 462 477 456 335 269 162 165 455 502 468 453 439 503, 411 334 509 494 461 472 488 285 374 342 372 402 485 501 434 385, 172 440 408 510 495 504 491 473 262 451 498 466 452 406 386 326, 475 174 409 511 492 507 271 366 164 481 449 486 471 390 340 260, 463 415 399 446 398 447 410 430 420 422 464 438 388 405 389 484, 414 412 396 474 458 442 428 394 423 421 448 384 487 436 437 404, 413 445 459 431 270 395 429 427 416 418 480 432 401 400 496 407, 444 506 443 393 489 286 424 426 417 483 261 358 433 403 465 391, 392 350 284 457 380 382 300 425 419 263 327 309 277 499 482 497, 490 505 268 173 318 301 282 264 259 257 256 258 308 356 435 387, 287 348 302 170 319 365 280 266 295 359 294 167 279 467 166 276, 364 317 316 281 299 330 314 298 275 288 304 273 160 292 310 324, 441 332 267 346 315 313 312 296 291 289 320 305 306 272 293 325, 303 383 265 362 378 10 361 297 355 290 352 370 336 353 311 274, 283 171 328 360 169 329 381 376 371 307 354 321 3 163 369 368, 367 379 347 8 331 344 345 377 35 339 323 375 337 0 322 373, 168 363 58 11 42 333 40 41 19 39 32 338 17 48 161 2, 74 26 27 45 43 24 56 57 50 34 33 38 96 16 49 1, 126 44 123 59 122 9 25 120 115 99 113 103 97 102 53 240, 62 90 46 106 107 104 105 121 114 51 67 65 112 64 71 227, 201 91 47 124 75 72 125 73 83 98 18 81 36 80 52 7, 12 28 109 29 61 60 127 89 82 66 119 37 23 20 211 21, 219 251 31 92 249 110 111 88 117 118 55 100 243 6 241 209, 203 153 185 94 76 108 77 93 101 87 69 54 70 68 179 147, 136 253 235 349 217 13 248 95 85 116 22 225 193 226 4 129, 222 351 15 184 78 232 200 79 86 242 84 146 195 178 215 181, 191 220 236 255 152 239 252 216 194 210 245 244 246 198 148 130, 143 159 223 204 206 238 254 207 213 197 229 212 196 214 149 133, 234 137 218 139 508 157 237 14 177 208 183 128 470 199 230 5, 187 205 189 478 476 154 186 30 231 341 192 151 150 180 228 145, 155 156 140 142 141 202 250 63 224 176 144 454 500 134 131 247, 221 188 190 158 460 138 175 233 357 278 450 135 469 182 132 343]
	[48 37 96 33 306 64 5 308 186 60 90 441 41 123 45 233, 225 112 113 339 161 129 224 240 250 26 10 42 40 107 61 127, 179 103 39 32 17 241 341 69 126 74 58 347 169 59 11 235, 343 16 0 1 65 81 80 21 63 124 122 43 345 171 106 44, 35 49 51 99 98 34 114 50 89 25 73 9 105 120 121 57, 163 3 115 53 83 66 2 18 72 185 88 249 91 75 104 56, 97 67 117 119 55 116 82 54 93 13 77 232 111 8 125 109, 19 227 131 102 226 38 118 52 153 248 95 29 137 24 108 27, 101 100 36 195 178 87 242 6 22 217 79 201 184 76 47 349, 243 68 85 23 84 70 194 86 216 152 200 136 15 219 187 251, 7 211 245 4 247 20 130 146 221 205 155 253 189 92 139 110, 193 147 229 183 230 215 210 246 157 223 236 239 255 237 12 203, 71 231 181 199 244 198 150 182 204 207 252 141 78 28 31 351, 176 144 135 197 213 151 134 214 159 220 238 222 254 94 202 234, 145 128 192 228 149 196 212 148 206 143 140 191 188 218 14 46, 310 209 342 208 133 166 132 180 156 158 142 174 154 30 138 62, 374 450 278 438 471 406 164 470 478 479 476 477 190 172 397 472, 262 402 466 502 390 454 468 404 462 415 412 460 413 461 408 456, 434 386 326 340 407 500 469 452 414 350 463 399 396 492 175 392, 279 439 276 422 486 455 405 464 398 510 494 511 508 495 411 509, 358 167 503 436 391 453 388 484 446 430 474 444 428 445 348 332, 387 260 418 501 437 400 448 389 286 410 447 284 493 287 475 443, 165 467 324 485 487 423 384 420 394 458 431 334 395 268 424 303, 419 356 435 403 277 496 421 401 270 382 490 429 459 366 507 267, 357 481 272 327 449 432 465 318 426 442 506 380 170 491 383 425, 293 295 160 336 263 385 480 416 316 302 319 300 427 301 296 365, 353 288 256 359 325 497 433 261 282 266 346 317 330 315 312 297, 305 289 352 321 257 273 320 417 298 314 378 362 299 376 379 377, 451 292 373 371 354 309 375 372 457 173 367 281 265 344 440 271, 499 368 307 369 322 258 311 482 285 488 393 328 329 331 280 364, 483 304 291 323 290 338 274 294 335 504 168 505 363 360 264 489, 275 259 337 355 370 177 162 498 409 473 269 333 361 313 381 283]
	[48 37 96 33 306 64 5 308 186 60 90 441 41 123 45 233, 225 112 113 339 161 129 224 240 250 26 10 42 40 107 61 127, 179 103 39 32 17 241 341 69 126 74 58 347 169 59 11 235, 343 16 0 1 65 81 80 21 63 124 122 43 345 171 106 44, 35 49 51 99 98 34 114 50 89 25 73 9 105 120 121 57, 163 3 115 53 83 66 2 18 72 185 88 249 91 75 104 56, 97 67 117 119 55 116 82 54 93 13 77 232 111 8 125 109, 19 227 131 102 226 38 118 52 153 248 95 29 137 24 108 27, 101 100 36 195 178 87 242 6 22 217 79 201 184 76 47 349, 243 68 85 23 84 70 194 86 216 152 200 136 15 219 187 251, 7 211 245 4 247 20 130 146 221 205 155 253 189 92 139 110, 193 147 229 183 230 215 210 246 157 223 236 239 255 237 12 203, 71 231 181 199 244 198 150 182 204 207 252 141 78 28 31 351, 176 144 135 197 213 151 134 214 159 220 238 222 254 94 202 234, 145 128 192 228 149 196 212 148 206 143 140 191 188 218 14 46, 310 209 342 208 133 166 132 180 156 158 142 174 154 30 138 62, 374 450 278 438 471 406 164 470 478 479 476 477 190 172 397 472, 262 402 466 502 390 454 468 404 462 415 412 460 413 461 408 456, 434 386 326 340 407 500 469 452 414 350 463 399 396 492 175 392, 279 439 276 422 486 455 405 464 398 510 494 511 508 495 411 509, 358 167 503 436 391 453 388 484 446 430 474 444 428 445 348 332, 387 260 418 501 437 400 448 389 286 410 447 284 493 287 475 443, 165 467 324 485 487 423 384 420 394 458 431 334 395 268 424 303, 419 356 435 403 277 496 421 401 270 382 490 429 459 366 507 267, 357 481 272 327 449 432 465 318 426 442 506 380 170 491 383 425, 293 295 160 336 263 385 480 416 316 302 319 300 427 301 296 365, 353 288 256 359 325 497 433 261 282 266 346 317 330 315 312 297, 305 289 352 321 257 273 320 417 298 314 378 362 299 376 379 377, 451 292 373 371 354 309 375 372 457 173 367 281 265 344 440 271, 499 368 307 369 322 258 311 482 285 488 393 328 329 331 280 364, 483 304 291 323 290 338 274 294 335 504 168 505 363 360 264 489, 275 259 337 355 370 177 162 498 409 473 269 333 361 313 381 283]
	[48 37 96 33 306 64 5 308 186 60 90 441 41 123 45 233, 225 112 113 339 161 129 224 240 250 26 10 42 40 107 61 127, 179 103 39 32 17 241 341 69 126 74 58 347 169 59 11 235, 343 16 0 1 65 81 80 21 63 124 122 43 345 171 106 44, 35 49 51 99 98 34 114 50 89 25 73 9 105 120 121 57, 163 3 115 53 83 66 2 18 72 185 88 249 91 75 104 56, 97 67 117 119 55 116 82 54 93 13 77 232 111 8 125 109, 19 227 131 102 226 38 118 52 153 248 95 29 137 24 108 27, 101 100 36 195 178 87 242 6 22 217 79 201 184 76 47 349, 243 68 85 23 84 70 194 86 216 152 200 136 15 219 187 251, 7 211 245 4 247 20 130 146 221 205 155 253 189 92 139 110, 193 147 229 183 230 215 210 246 157 223 236 239 255 237 12 203, 71 231 181 199 244 198 150 182 204 207 252 141 78 28 31 351, 176 144 135 197 213 151 134 214 159 220 238 222 254 94 202 234, 145 128 192 228 149 196 212 148 206 143 140 191 188 218 14 46, 310 209 342 208 133 166 132 180 156 158 142 174 154 30 138 62, 374 450 278 438 471 406 164 470 478 479 476 477 190 172 397 472, 262 402 466 502 390 454 468 404 462 415 412 460 413 461 408 456, 434 386 326 340 407 500 469 452 414 350 463 399 396 492 175 392, 279 439 276 422 486 455 405 464 398 510 494 511 508 495 411 509, 358 167 503 436 391 453 388 484 446 430 474 444 428 445 348 332, 387 260 418 501 437 400 448 389 286 410 447 284 493 287 475 443, 165 467 324 485 487 423 384 420 394 458 431 334 395 268 424 303, 419 356 435 403 277 496 421 401 270 382 490 429 459 366 507 267, 357 481 272 327 449 432 465 318 426 442 506 380 170 491 383 425, 293 295 160 336 263 385 480 416 316 302 319 300 427 301 296 365, 353 288 256 359 325 497 433 261 282 266 346 317 330 315 312 297, 305 289 352 321 257 273 320 417 298 314 378 362 299 376 379 377, 451 292 373 371 354 309 375 372 457 173 367 281 265 344 440 271, 499 368 307 369 322 258 311 482 285 488 393 328 329 331 280 364, 483 304 291 323 290 338 274 294 335 504 168 505 363 360 264 489, 275 259 337 355 370 177 162 498 409 473 269 333 361 313 381 283]
	[48 37 96 33 306 64 5 308 186 60 90 441 41 123 45 233, 225 112 113 339 161 129 224 240 250 26 10 42 40 107 61 127, 179 103 39 32 17 241 341 69 126 74 58 347 169 59 11 235, 343 16 0 1 65 81 80 21 63 124 122 43 345 171 106 44, 35 49 51 99 98 34 114 50 89 25 73 9 105 120 121 57, 163 3 115 53 83 66 2 18 72 185 88 249 91 75 104 56, 97 67 117 119 55 116 82 54 93 13 77 232 111 8 125 109, 19 227 131 102 226 38 118 52 153 248 95 29 137 24 108 27, 101 100 36 195 178 87 242 6 22 217 79 201 184 76 47 349, 243 68 85 23 84 70 194 86 216 152 200 136 15 219 187 251, 7 211 245 4 247 20 130 146 221 205 155 253 189 92 139 110, 193 147 229 183 230 215 210 246 157 223 236 239 255 237 12 203, 71 231 181 199 244 198 150 182 204 207 252 141 78 28 31 351, 176 144 135 197 213 151 134 214 159 220 238 222 254 94 202 234, 145 128 192 228 149 196 212 148 206 143 140 191 188 218 14 46, 310 209 342 208 133 166 132 180 156 158 142 174 154 30 138 62, 374 450

TABLE XI
PROPOSED λ_{el} AND λ_{ol} FOR 512-QAM.

λ_{el}	[(172 428) (168 424) (162 418) (165 421) (175 431) (173 429) (164 420) (170 426), (160 416) (167 423) (161 417) (42 298) (43 299) (169 425) (41 297) (57 313), (35 291) (33 289) (32 288) (1 257) (64 320) (177 433) (10 266) (58 314), (171 427) (122 378) (59 315) (123 379) (40 296) (121 377) (51 307) (49 305), (163 419) (96 352) (65 321) (17 273) (241 497) (80 336) (90 346) (74 330), (106 362) (45 301) (107 363) (56 312) (105 361) (120 376) (34 290) (99 355), (97 353) (113 369) (37 293) (39 295) (103 359) (69 325) (124 380) (235 491), (61 317) (11 267) (109 365) (75 331) (104 360) (9 265) (50 306) (98 354), (115 371) (19 275) (48 304) (112 368) (81 337) (7 263) (63 319) (44 300), (127 383) (233 489) (125 381) (91 347) (73 329) (25 281) (89 345) (114 370), (3 259) (67 323) (225 481) (0 256) (16 272) (100 356) (139 395) (110 366), (47 303) (27 283) (108 364) (8 264) (88 344) (72 328) (66 322) (83 339), (53 309) (227 483) (101 357) (243 499) (179 435) (71 327) (12 268) (92 348), (251 507) (24 280) (111 367) (249 505) (185 441) (2 258) (117 373) (116 372), (119 375) (195 451) (131 387) (68 324) (211 467) (189 445) (219 475) (76 332), (187 443) (137 393) (232 488) (77 333) (93 349) (18 274) (82 338) (55 311), (226 482) (102 358) (85 341) (4 260) (229 485) (255 511) (253 509) (15 271), (201 457) (29 285) (95 351) (13 269) (54 310) (242 498) (118 374) (38 294), (87 343) (23 279) (36 292) (247 503) (230 486) (252 508) (239 495) (155 411), (136 392) (184 440) (79 335) (248 504) (153 409) (52 308) (6 262) (178 434), (70 326) (84 340) (20 276) (244 500) (198 454) (238 494) (207 463) (141 397), (205 461) (152 408) (200 456) (216 472) (217 473) (86 342) (22 278) (194 450), (130 386) (210 466) (215 471) (150 406) (212 468) (156 412) (159 415) (206 462), (220 476) (236 492) (204 460) (223 479) (221 477) (157 413) (146 402) (246 502), (182 438) (134 390) (214 470) (148 404) (180 436) (203 459) (94 350) (154 410), (142 398) (174 430) (14 270) (46 302) (234 490) (21 277) (176 432) (144 400), (208 464) (133 389) (149 405) (147 403) (193 449) (31 287) (78 334) (188 444), (158 414) (218 474) (138 394) (250 506) (126 382) (129 385) (128 384) (228 484), (166 422) (197 453) (231 487) (28 284) (254 510) (222 478) (140 396) (190 446), (202 458) (186 442) (26 282) (5 261) (240 496) (209 465) (135 391) (196 452), (213 469) (199 455) (245 501) (237 493) (191 447) (143 399) (30 286) (62 318), (60 316) (224 480) (145 401) (192 448) (132 388) (151 407) (183 439) (181 437)]
	[(225 481) (19 275) (163 419) (33 289) (64 320) (177 433) (60 316) (58 314), (42 298) (57 313) (40 296) (56 312) (125 381) (179 435) (48 304) (113 369), (49 305) (161 417) (17 273) (241 497) (224 480) (126 382) (10 266) (90 346), (43 299) (41 297) (123 379) (45 301) (103 359) (112 368) (37 293) (97 353), (1 257) (65 321) (80 336) (129 385) (234 490) (26 282) (74 330) (171 427), (169 425) (107 363) (11 267) (127 383) (69 325) (0 256) (39 295) (32 288), (96 352) (81 337) (63 319) (124 380) (106 362) (122 378) (59 315) (61 317), (235 491) (44 300) (35 291) (34 290) (51 307) (98 354) (114 370) (66 322), (89 345) (50 306) (185 441) (72 328) (25 281) (73 329) (9 265) (120 376), (121 377) (99 355) (3 259) (227 483) (53 309) (83 339) (55 311) (82 338), (18 274) (2 258) (249 505) (88 344) (111 367) (8 264) (91 347) (104 360), (105 361) (115 371) (67 323) (117 373) (116 372) (38 294) (242 498) (118 374), (13 269) (93 349) (77 333) (232 488) (137 393) (24 280) (27 283) (109 365), (75 331) (101 357) (119 375) (226 482) (102 358) (178 434) (52 308) (153 409), (54 310) (248 504) (29 285) (95 351) (184 440) (108 364) (47 303) (233 489), (243 499) (131 387) (195 451) (23 279) (70 326) (87 343) (6 262) (194 450), (217 473) (79 335) (201 457) (15 271) (76 332) (187 443) (16 272) (36 292), (85 341) (211 467) (84 340) (130 386) (146 402) (86 342) (22 278) (200 456), (216 472) (136 392) (219 475) (12 268) (92 348) (251 507) (100 356) (71 327), (68 324) (4 260) (247 503) (20 276) (210 466) (157 413) (221 477) (152 408), (155 411) (253 509) (189 445) (237 493) (139 395) (110 366) (7 263) (193 449), (229 485) (245 501) (244 500) (215 471) (134 390) (246 502) (205 461) (236 492), (141 397) (239 495) (255 511) (28 284) (31 287) (203 459) (5 261) (21 277), (181 437) (199 455) (230 486) (198 454) (150 406) (182 438) (223 479) (220 476), (207 463) (252 508) (254 510) (78 334) (94 350) (250 506) (240 496) (147 403), (231 487) (197 453) (183 439) (151 407) (212 468) (214 470) (204 460) (206 462), (238 494) (191 447) (188 444) (218 474) (14 270) (46 302) (176 432) (128 384), (208 464) (149 405) (213 469) (196 452) (132 388) (148 404) (159 415) (156 412), (222 478) (142 398) (190 446) (154 410) (202 458) (186 442) (209 465) (144 400), (228 484) (135 391) (133 389) (166 422) (164 420) (180 436) (143 399) (140 396), (158 414) (174 430) (30 286) (138 394) (62 318) (145 401) (192 448) (167 423), (172 428) (175 431) (165 421) (173 429) (170 426) (160 416) (162 417) (168 424) (171 427)
	[(225 481) (19 275) (163 419) (33 289) (64 320) (177 433) (60 316) (58 314), (42 298) (57 313) (40 296) (56 312) (125 381) (179 435) (48 304) (113 369), (49 305) (161 417) (17 273) (241 497) (224 480) (126 382) (10 266) (90 346), (43 299) (41 297) (123 379) (45 301) (103 359) (112 368) (37 293) (97 353), (1 257) (65 321) (80 336) (129 385) (234 490) (26 282) (74 330) (171 427), (169 425) (107 363) (11 267) (127 383) (69 325) (0 256) (39 295) (32 288), (96 352) (81 337) (63 319) (124 380) (106 362) (122 378) (59 315) (61 317), (235 491) (44 300) (35 291) (34 290) (51 307) (98 354) (114 370) (66 322), (89 345) (50 306) (185 441) (72 328) (25 281) (73 329) (9 265) (120 376), (121 377) (99 355) (3 259) (227 483) (53 309) (83 339) (55 311) (82 338), (18 274) (2 258) (249 505) (88 344) (111 367) (8 264) (91 347) (104 360), (105 361) (115 371) (67 323) (117 373) (116 372) (38 294) (242 498) (118 374), (13 269) (93 349) (77 333) (232 488) (137 393) (24 280) (27 283) (109 365), (75 331) (101 357) (119 375) (226 482) (102 358) (178 434) (52 308) (153 409), (54 310) (248 504) (29 285) (95 351) (184 440) (108 364) (47 303) (233 489), (243 499) (131 387) (195 451) (23 279) (70 326) (87 343) (6 262) (194 450), (217 473) (79 335) (201 457) (15 271) (76 332) (187 443) (16 272) (36 292), (85 341) (211 467) (84 340) (130 386) (146 402) (86 342) (22 278) (200 456), (216 472) (136 392) (219 475) (12 268) (92 348) (251 507) (100 356) (71 327), (68 324) (4 260) (247 503) (20 276) (210 466) (157 413) (221 477) (152 408), (155 411) (253 509) (189 445) (237 493) (139 395) (110 366) (7 263) (193 449), (229 485) (245 501) (244 500) (215 471) (134 390) (246 502) (205 461) (236 492), (141 397) (239 495) (255 511) (28 284) (31 287) (203 459) (5 261) (21 277), (181 437) (199 455) (230 486) (198 454) (150 406) (182 438) (223 479) (220 476), (207 463) (252 508) (254 510) (78 334) (94 350) (250 506) (240 496) (147 403), (231 487) (197 453) (183 439) (151 407) (212 468) (214 470) (204 460) (206 462), (238 494) (191 447) (188 444) (218 474) (14 270) (46 302) (176 432) (128 384), (208 464) (149 405) (213 469) (196 452) (132 388) (148 404) (159 415) (156 412), (222 478) (142 398) (190 446) (154 410) (202 458) (186 442) (209 465) (144 400), (228 484) (135 391) (133 389) (166 422) (164 420) (180 436) (143 399) (140 396), (158 414) (174 430) (30 286) (138 394) (62 318) (145 401) (192 448) (167 423), (172 428) (175 431) (165 421) (173 429) (170 426) (160 416) (162 417) (168 424) (171 427)

TABLE XII
PROPOSED λ_{er} FOR 1024-QAM.

λ_{er}	[674	195	226	193	197	229	67	225	129	163	161	165	97	69	203	65,
	182	54	252	222	220	180	118	176	86	151	148	150	247	246	214	212,
	194	199	227	231	131	133	200	99	234	202	37	101	1	33	235	201,
	158	156	254	22	52	470	23	20	116	183	144	146	215	242	244	213,
	192	228	224	162	66	64	3	5	35	451	483	139	485	481	449	233,
	406	190	404	407	502	223	48	50	468	112	178	87	240	245	210	208,
	196	230	130	167	205	237	450	487	453	389	385	77	72	171	137	169,
	438	188	94	436	400	159	191	500	16	255	114	179	181	84	243	694,
	198	128	98	68	232	39	448	141	138	419	355	421	74	417	75	73,
	126	30	124	432	434	402	92	184	496	18	248	119	82	147	149	662,
	134	135	103	96	239	0	136	173	104	109	13	106	323	353	107	105,
	62	278	28	342	374	127	95	186	471	498	503	55	221	80	145	209,
	132	160	71	2	455	482	170	423	359	322	45	10	11	325	357	321,
	60	310	304	476	31	368	370	439	403	435	152	464	253	19	115	211,
	166	164	7	32	480	387	168	324	320	8	456	257	461	491	9	41,
	412	510	306	308	274	276	372	343	336	340	189	157	51	250	177	241,
	70	100	4	34	452	418	327	356	495	490	42	261	493	293	43	457,
	446	508	478	272	279	307	63	56	375	371	120	154	466	218	216	83,
	102	204	207	484	386	76	354	260	40	291	488	458	289	459	393	489,
	414	444	447	408	479	511	275	472	58	338	122	405	499	469	21	117,
	238	36	143	175	384	79	111	47	259	295	397	429	427	363	361	425,
	284	286	415	440	442	410	311	504	506	24	125	401	155	467	53	85,
	6	486	454	420	12	15	352	292	258	392	426	394	395	301	331	329,
	318	380	314	348	445	413	509	305	61	26	433	437	187	501	49	113,
	236	140	391	416	78	326	263	256	463	431	424	365	269	328	265	297,
	316	280	312	376	443	411	309	477	474	273	29	93	90	88	251	17,
	38	206	388	108	358	294	460	290	288	399	268	367	271	360	299	267,
	287	350	383	315	282	378	441	475	277	507	27	339	123	497	219	81,
	673	142	172	422	14	44	494	492	428	270	364	332	303	264	266	330,
	382	319	317	283	313	379	346	409	59	373	341	369	185	153	249	217,
	581	174	390	110	46	262	396	398	430	462	302	300	333	362	298	296,
	351	285	381	281	347	344	377	473	505	25	337	121	91	465	702	566,
	609	745	961	681	585	617	833	553	521	969	335	873	366	777	334	809,
	829	831	349	828	830	345	798	924	57	572	574	542	89	638	918	534,
	577	713	993	649	837	869	865	555	805	1001	939	843	937	875	813	811,
	825	827	792	826	796	892	862	956	958	926	822	790	636	700	670	764,
	677	747	997	619	587	835	523	971	1003	905	845	841	781	815	779	810,
	793	797	824	799	794	894	952	927	816	818	1022	540	944	950	668	766,
	579	513	545	683	933	525	522	773	1005	941	907	877	842	776	778	808,
	893	891	795	895	888	860	959	954	1020	820	990	543	606	916	1014	732,
	741	715	651	586	929	621	557	968	973	769	801	840	879	783	812	780,
	953	859	856	863	957	890	920	784	788	786	791	854	912	948	564	734,
	611	613	549	584	897	589	970	554	807	1000	909	906	872	874	876	814,
	921	889	858	955	923	922	823	991	575	988	882	886	919	671	560	688,
	641	547	963	995	901	871	867	520	1007	803	943	938	904	936	847	782,
	861	1021	821	989	925	984	1016	819	787	880	639	914	946	735	982	630,
	705	714	965	650	931	618	834	1002	552	771	975	844	768	911	940	878,
	857	987	789	817	573	986	1018	570	568	884	604	1008	703	980	532	656,
	737	578	517	999	685	616	836	832	866	559	772	770	775	1004	908	846,
	910	1017	1019	785	536	1023	887	852	855	915	607	983	1012	562	535	660,
	675	746	515	962	749	653	935	899	839	868	804	972	802	800	974	942,
	985	569	539	538	541	883	850	848	947	951	696	1010	767	624	628	663,
	709	643	712	717	744	682	960	996	623	591	864	527	838	1006	556	774,
	885	537	571	851	945	637	634	632	669	664	698	528	567	631	598	690,
	739	707	645	551	514	994	648	680	687	898	588	870	524	806	526	558,
	849	853	881	605	913	600	917	976	701	733	765	530	596	599	658	692,
	679	704	610	576	615	751	967	512	930	964	655	896	903	590	620	633,
	601	603	635	602	949	667	666	978	760	1015	531	762	626	752	727	695,
	706	642	740	580	583	546	612	516	992	719	966	932	928	900	902	622,
	977	697	665	1009	699	979	981	728	730	563	592	659	720	722	754	759,
	738	736	743	676	708	608	644	519	544	548	716	998	934	652	654	684,
	761	729	1013	731	529	1011	565	533	627	594	657	661	691	724	756	726,
	678	672	742	710	711	646	640	647	582	614	550	518	718	748	686	750,
	593	625	763	561	597	629	595	721	689	753	723	725	755	757	693	758]

TABLE XIII
PROPOSED λ_{or} FOR 1024-QAM.

λ_{or}	[829	825	827	797	793	893	891	889	856	859	921	861	987	857	1017	985,
	910	846	942	908	940	878	782	876	814	783	812	778	808	810	811	809,
	831	792	824	795	953	957	955	858	1021	821	789	1019	571	569	537	849,
	774	556	1006	974	802	911	1004	844	847	936	874	780	776	815	779	334,
	349	826	799	895	863	923	817	573	989	541	785	539	885	881	853	633,
	558	526	806	524	972	800	775	772	768	904	938	872	879	781	875	813,
	828	796	794	890	925	1016	984	986	538	536	945	851	605	635	603	697,
	601	590	620	870	838	527	864	804	770	975	771	943	840	842	843	777,
	345	888	860	922	823	1023	570	887	883	637	913	600	602	1009	665	902,
	622	900	928	903	896	588	623	866	868	559	554	803	906	941	939	366,
	830	894	920	991	819	1018	848	850	632	917	949	667	699	731	1013	977,
	654	684	934	932	655	898	591	899	839	832	552	807	1000	909	907	937,
	892	959	954	575	787	568	855	634	947	976	666	979	1011	561	729	761,
	686	652	966	719	964	687	930	680	935	836	1002	1007	970	801	845	877,
	798	784	788	880	884	882	852	701	669	978	1015	728	981	565	529	593,
	718	998	548	544	992	996	648	960	653	931	616	834	520	968	769	841,
	927	1020	791	543	639	607	915	951	664	765	733	730	533	595	763	625,
	748	518	716	516	751	967	512	682	685	901	618	871	867	557	1005	873,
	952	820	786	604	914	696	1008	1010	980	760	531	762	563	627	629	597,
	750	519	612	615	546	994	514	962	749	650	897	525	522	773	973	905,
	862	818	988	886	912	703	698	528	530	567	596	659	592	594	657	721,
	550	614	582	608	583	551	744	717	999	965	584	589	621	835	971	805,
	816	1022	990	854	946	671	983	1012	767	631	626	599	661	720	753	689,
	644	647	640	676	580	610	712	515	517	549	995	586	929	865	523	1003,
	924	822	540	636	919	948	735	560	532	624	752	658	691	722	725	723,
	646	710	711	708	645	576	746	714	547	513	963	651	933	837	555	1001,
	956	572	542	944	916	564	982	732	562	628	598	663	727	724	755	693,
	742	743	740	642	707	578	705	611	613	997	545	683	587	619	521	969,
	958	926	638	606	950	668	1014	764	734	535	656	660	754	756	759	757,
	736	672	679	704	709	643	641	579	747	715	993	961	649	585	869	553,
	57	790	89	700	918	702	670	566	766	534	630	690	692	695	758	726,
	678	738	706	739	675	737	677	673	581	609	713	745	681	617	833	398,
	25	574	121	91	465	249	219	217	81	113	688	241	662	694	208	213,
	194	674	196	230	198	166	741	6	38	577	142	390	172	110	262	430,
	505	337	369	185	153	497	49	251	17	85	117	83	209	210	242	212,
	195	192	199	228	134	132	70	102	236	238	140	174	388	14	46	396,
	473	341	93	123	90	467	501	53	218	115	177	145	211	245	247	214,
	227	226	231	224	128	135	164	7	204	486	206	454	422	108	44	428,
	373	27	339	437	187	88	469	21	19	216	80	149	243	240	215	244,
	193	197	131	162	130	98	160	4	207	36	143	391	420	78	294	492,
	59	507	433	371	401	155	499	51	250	82	181	147	146	144	148	246,
	225	229	133	64	167	68	71	100	32	452	175	384	416	358	494	462,
	409	277	29	125	122	405	466	253	248	221	179	84	183	178	176	151,
	129	67	99	163	66	103	96	239	34	484	386	418	12	326	460	288,
	475	305	273	26	120	154	157	464	55	119	114	87	116	118	86	150,
	182	161	165	200	205	232	2	455	0	480	76	111	15	292	290	270,
	377	477	474	24	338	435	189	498	503	16	255	468	112	220	22	180,
	65	97	234	202	5	237	39	448	482	168	79	354	352	263	463	302,
	346	309	61	506	375	340	186	152	471	18	50	23	20	52	222	54,
	69	1	101	37	35	3	487	136	170	423	356	260	495	256	399	335,
	379	441	509	504	58	336	439	403	184	496	500	223	48	156	254	252,
	235	203	33	483	453	450	138	141	387	327	320	40	259	258	431	364,
	313	378	411	472	307	56	372	127	92	402	191	159	470	404	158	406,
	201	449	485	451	385	389	173	355	104	324	47	291	295	392	332	300,
	347	344	443	511	311	343	276	95	370	434	400	407	436	502	188	190,
	233	481	139	171	421	109	419	106	359	322	490	488	426	367	268	303,
	281	283	445	413	442	410	275	63	274	368	31	28	94	432	438	73,
	169	137	75	72	417	77	13	10	8	456	42	397	424	365	271	333,
	381	315	282	376	415	479	440	408	279	476	374	342	310	124	30	126,
	105	107	323	353	74	45	257	261	461	289	429	394	269	360	264	362,
	285	317	383	312	314	348	380	447	272	508	308	304	306	60	278	62,
	321	357	9	325	11	491	293	493	458	427	395	328	301	299	266	298,
	351	382	319	287	350	280	318	316	284	286	478	444	510	414	446	412,
	457	41	489	43	459	425	393	361	363	331	265	329	297	267	330	296]

TABLE XIV
PROPOSED λ_{el} FOR 1024-QAM.

λ_{el}	[(195 707) (226 738) (193 705) (197 709) (229 741) (67 579) (225 737) (129 641),
	(163 675) (161 673) (165 677) (97 609) (69 581) (203 715) (65 577) (182 694),
	(54 566) (252 764) (222 734) (220 732) (180 692) (118 630) (176 688) (86 598),
	(151 663) (148 660) (150 662) (247 759) (246 758) (214 726) (212 724) (194 706),
	(199 711) (227 739) (231 743) (131 643) (133 645) (200 712) (99 611) (234 746),
	(202 714) (37 549) (101 613) (1 513) (33 545) (235 747) (201 713) (158 670),
	(156 668) (254 766) (22 534) (52 564) (470 982) (23 535) (20 532) (116 628),
	(183 695) (144 656) (146 658) (215 727) (242 754) (244 756) (213 725) (192 704),
	(228 740) (224 736) (162 674) (66 578) (64 576) (3 515) (5 517) (35 547),
	(451 963) (483 995) (139 651) (485 997) (481 993) (449 961) (233 745) (406 918),
	(190 702) (404 916) (407 919) (502 1014) (223 735) (48 560) (50 562) (468 980),
	(112 624) (178 690) (87 599) (240 752) (245 757) (210 722) (208 720) (196 708),
	(230 742) (130 642) (167 679) (205 717) (237 749) (450 962) (487 999) (453 965),
	(389 901) (385 897) (77 589) (72 584) (171 683) (137 649) (169 681) (438 950),
	(188 700) (94 606) (436 948) (400 912) (159 671) (191 703) (500 1012) (16 528),
	(255 767) (114 626) (179 691) (181 693) (84 596) (243 755) (198 710) (128 640),
	(98 610) (68 580) (232 744) (39 551) (448 960) (141 653) (138 650) (419 931),
	(355 867) (421 933) (74 586) (417 929) (75 587) (73 585) (126 638) (30 542),
	(124 636) (432 944) (434 946) (402 914) (92 604) (184 696) (496 1008) (18 530),
	(248 760) (119 631) (82 594) (147 659) (149 661) (134 646) (135 647) (103 615),
	(96 608) (239 751) (0 512) (136 648) (173 685) (104 616) (109 621) (13 525),
	(106 618) (323 835) (353 865) (107 619) (105 617) (62 574) (278 790) (28 540),
	(342 854) (374 886) (127 639) (95 607) (186 698) (471 983) (498 1010) (503 1015),
	(55 567) (221 733) (80 592) (145 657) (209 721) (132 644) (160 672) (71 583),
	(2 514) (455 967) (482 994) (170 682) (423 935) (359 871) (322 834) (45 557),
	(10 522) (11 523) (325 837) (357 869) (321 833) (60 572) (310 822) (304 816),
	(476 988) (31 543) (368 880) (370 882) (439 951) (403 915) (435 947) (152 664),
	(464 976) (253 765) (19 531) (115 627) (211 723) (166 678) (164 676) (7 519),
	(32 544) (480 992) (387 899) (168 680) (324 836) (320 832) (8 520) (456 968),
	(257 769) (461 973) (491 1003) (9 521) (41 553) (412 924) (510 1022) (306 818),
	(308 820) (274 786) (276 788) (372 884) (343 855) (336 848) (340 852) (189 701),
	(157 669) (51 563) (250 762) (177 689) (241 753) (70 582) (100 612) (4 516),
	(34 546) (452 964) (418 930) (327 839) (356 868) (495 1007) (490 1002) (42 554),
	(261 773) (493 1005) (293 805) (43 555) (457 969) (446 958) (508 1020) (478 990),
	(272 784) (279 791) (307 819) (63 575) (56 568) (375 887) (371 883) (120 632),
	(154 666) (466 978) (218 730) (216 728) (83 595) (102 614) (204 716) (207 719),
	(484 996) (386 898) (76 588) (354 866) (260 772) (40 552) (291 803) (488 1000),
	(458 970) (289 801) (459 971) (393 905) (489 1001) (414 926) (444 956) (447 959),
	(408 920) (479 991) (511 1023) (275 787) (472 984) (58 570) (338 850) (122 634),
	(405 917) (499 1011) (469 981) (21 533) (117 629) (238 750) (36 548) (143 655),
	(175 687) (384 896) (79 591) (111 623) (47 559) (259 771) (295 807) (397 909),
	(429 941) (427 939) (363 875) (361 873) (425 937) (284 796) (286 798) (415 927),
	(440 952) (442 954) (410 922) (311 823) (504 1016) (506 1018) (24 536) (125 637),
	(401 913) (155 667) (467 979) (53 565) (85 597) (6 518) (486 998) (454 966),
	(420 932) (12 524) (15 527) (352 864) (292 804) (258 770) (392 904) (426 938),
	(394 906) (395 907) (301 813) (331 843) (329 841) (318 830) (380 892) (314 826),
	(348 860) (445 957) (413 925) (509 1021) (305 817) (61 573) (26 538) (433 945),
	(437 949) (187 699) (501 1013) (49 561) (113 625) (236 748) (140 652) (391 903),
	(416 928) (78 590) (326 838) (263 775) (256 768) (463 975) (431 943) (424 936),
	(365 877) (269 781) (328 840) (265 777) (297 809) (316 828) (280 792) (312 824),
	(376 888) (443 955) (411 923) (309 821) (477 989) (474 986) (273 785) (29 541),
	(93 605) (90 602) (88 600) (251 763) (17 529) (38 550) (206 718) (388 900),
	(108 620) (358 870) (294 806) (460 972) (290 802) (288 800) (399 911) (268 780),
	(367 879) (271 783) (360 872) (299 811) (267 779) (287 799) (350 862) (383 895),
	(315 827) (282 794) (378 890) (441 953) (475 987) (277 789) (507 1019) (27 539),
	(339 851) (123 635) (497 1009) (219 731) (81 593) (142 654) (172 684) (422 934),
	(14 526) (44 556) (494 1006) (492 1004) (428 940) (270 782) (364 876) (332 844),
	(303 815) (264 776) (266 778) (330 842) (382 894) (319 831) (317 829) (283 795),
	(313 825) (379 891) (346 858) (409 921) (59 571) (373 885) (341 853) (369 881),
	(185 697) (153 665) (249 761) (217 729) (174 686) (390 902) (110 622) (46 558),
	(262 774) (396 908) (398 910) (430 942) (462 974) (302 814) (300 812) (333 845),
	(362 874) (298 810) (296 808) (351 863) (285 797) (381 893) (281 793) (347 859),
	(344 856) (377 889) (473 985) (505 1017) (25 537) (337 849) (121 633) (91 603),
	(465 977) (335 847) (366 878) (334 846) (349 861) (345 857) (57 569) (89 601)],

TABLE XV
PROPOSED λ_{ol} FOR 1024-QAM.

λ_{ol}	[(349 861) (334 846) (366 878) (345 857) (473 985) (398 910) (335 847) (505 1017),
	(57 569) (121 633) (91 603) (89 601) (465 977) (249 761) (217 729) (81 593),
	(113 625) (209 721) (208 720) (212 724) (195 707) (196 708) (198 710) (134 646),
	(102 614) (38 550) (142 654) (390 902) (422 934) (46 558) (396 908) (430 942),
	(377 889) (25 537) (337 849) (185 697) (153 665) (497 1009) (219 731) (49 561),
	(17 529) (85 597) (83 595) (211 723) (243 755) (210 722) (213 725) (214 726),
	(194 706) (199 711) (230 742) (135 647) (132 644) (166 678) (70 582) (6 518),
	(236 748) (140 652) (174 686) (110 622) (14 526) (262 774) (294 806) (302 814),
	(409 921) (341 853) (369 881) (123 635) (88 600) (501 1013) (53 565) (251 763),
	(117 629) (177 689) (145 657) (241 753) (245 757) (247 759) (242 754) (246 758),
	(226 738) (192 704) (228 740) (128 640) (160 672) (71 583) (164 676) (204 716),
	(238 750) (206 718) (388 900) (172 684) (108 620) (44 556) (494 1006) (428 940),
	(346 858) (373 885) (339 851) (93 605) (187 699) (499 1011) (467 979) (218 730),
	(216 728) (115 627) (181 693) (149 661) (240 752) (215 727) (244 756) (193 705),
	(227 739) (231 743) (224 736) (130 642) (162 674) (68 580) (100 612) (7 519),
	(36 548) (486 998) (454 966) (420 932) (78 590) (460 972) (492 1004) (462 974),
	(475 987) (59 571) (27 539) (433 945) (90 602) (155 667) (51 563) (21 533),
	(19 531) (82 594) (80 592) (84 596) (147 659) (146 658) (148 660) (150 662),
	(225 737) (197 709) (229 741) (131 643) (167 679) (103 615) (4 516) (32 544),
	(207 719) (484 996) (391 903) (416 928) (12 524) (326 838) (290 802) (270 782),
	(347 859) (507 1019) (29 541) (437 949) (401 913) (469 981) (466 978) (253 765),
	(250 762) (221 733) (179 691) (114 626) (144 656) (151 663) (86 598) (118 630),
	(67 579) (129 641) (133 645) (66 578) (98 610) (96 608) (239 751) (34 546),
	(455 967) (143 655) (175 687) (384 896) (358 870) (292 804) (288 800) (268 780),
	(379 891) (277 789) (273 785) (125 637) (122 634) (405 917) (157 669) (464 976),
	(55 567) (119 631) (112 624) (87 599) (183 695) (176 688) (180 692) (182 694),
	(161 673) (163 675) (99 611) (64 576) (3 515) (205 717) (232 744) (2 514),
	(452 964) (386 898) (418 930) (76 588) (15 527) (263 775) (258 770) (399 911),
	(344 856) (309 821) (61 573) (26 538) (371 883) (120 632) (154 666) (503 1015),
	(255 767) (248 760) (16 528) (468 980) (178 690) (116 628) (220 732) (22 534),
	(65 577) (165 677) (200 712) (234 746) (5 517) (237 749) (39 551) (0 512),
	(480 992) (168 680) (327 839) (79 591) (354 866) (256 768) (463 975) (364 876),
	(411 923) (441 953) (305 817) (506 1018) (24 536) (338 850) (189 701) (152 664),
	(496 1008) (498 1010) (18 530) (23 535) (20 532) (52 564) (222 734) (203 715),
	(97 609) (69 581) (101 613) (202 714) (487 999) (450 962) (448 960) (482 994),
	(170 682) (423 935) (111 623) (260 772) (352 864) (47 559) (431 943) (300 812),
	(313 825) (443 955) (477 989) (474 986) (58 570) (375 887) (340 852) (435 947),
	(471 983) (184 696) (50 562) (223 735) (502 1014) (254 766) (252 764) (54 566),
	(201 713) (1 513) (37 549) (483 995) (35 547) (138 650) (141 653) (136 648),
	(387 899) (324 836) (356 868) (40 552) (259 771) (392 904) (424 936) (332 844),
	(283 795) (376 888) (410 922) (504 1016) (472 984) (56 568) (336 848) (403 915),
	(439 951) (186 698) (500 1012) (191 703) (48 560) (470 982) (158 670) (156 668),
	(235 747) (33 545) (485 997) (451 963) (453 965) (389 901) (173 685) (104 616),
	(359 871) (320 832) (495 1007) (490 1002) (291 803) (426 938) (367 879) (271 783),
	(381 893) (378 890) (413 925) (509 1021) (275 787) (343 855) (372 884) (370 882),
	(127 639) (92 604) (402 914) (159 671) (407 919) (400 912) (404 916) (233 745),
	(481 993) (406 918) (190 702) (139 651) (385 897) (419 931) (109 621) (355 867),
	(322 834) (8 520) (456 968) (295 807) (488 1000) (365 877) (269 781) (333 845),
	(317 829) (281 793) (282 794) (445 957) (311 823) (307 819) (63 575) (276 788),
	(95 607) (368 880) (432 944) (434 946) (94 606) (124 636) (436 948) (449 961),
	(137 649) (438 950) (171 683) (417 929) (72 584) (421 933) (106 618) (13 525),
	(45 557) (261 773) (42 554) (397 909) (394 906) (301 813) (303 815) (264 776),
	(383 895) (315 827) (314 826) (348 860) (442 954) (408 920) (511 1023) (274 786),
	(308 820) (31 543) (374 886) (342 854) (28 540) (30 542) (73 585) (188 700),
	(169 681) (75 587) (107 619) (74 586) (323 835) (77 589) (10 522) (257 769),
	(493 1005) (461 973) (429 941) (427 939) (395 907) (265 777) (360 872) (298 810),
	(285 797) (319 831) (280 792) (312 824) (286 798) (440 952) (479 991) (279 791),
	(272 784) (304 816) (476 988) (306 818) (310 822) (60 572) (105 617) (62 574),
	(278 790) (126 638) (353 865) (357 869) (11 523) (325 837) (491 1003) (293 805),
	(289 801) (458 970) (393 905) (331 843) (328 840) (299 811) (362 874) (296 808),
	(351 863) (382 894) (287 799) (350 862) (380 892) (318 830) (284 796) (415 927),
	(447 959) (478 990) (444 956) (508 1020) (457 969) (510 1022) (41 553) (9 521),
	(321 833) (412 924) (489 1001) (446 958) (414 926) (43 555) (425 937) (361 873),
	(459 971) (363 875) (329 841) (297 809) (316 828) (267 779) (266 778) (330 842)],

ACKNOWLEDGMENT

REFERENCES

- [1] G. Ungerboeck, "Channel coding with multilevel/phase signals," *IEEE Trans. Inform. Theory*, vol. IT-28, pp. 5567, Jan. 1982..
- [2] E. Zehavi, "8-PSK trellis codes for a Rayleigh channel," *IEEE Trans. Commun.*, vol. 40, pp. 873-884, May 1992.
- [3] X. Li and J. A. Ritcey, "Bit-interleaved coded modulation with iterative decoding," *IEEE Commun. Lett.*, vol. 1, pp. 169-171, Nov. 1997.
- [4] S. Ten Brink, J. Speidel, and R.-H. Yan, "Iterative demapping for QPSK modulation," *IEE Electron. Lett.*, vol. 34, pp. 1459-1460, Jul. 1998.
- [5] S. Benedetto, G. Montorsi, D. Divsalar, and F. Pollara, "Soft-input soft-output modules for the construction and distributed iterative decoding of code networks," *Eur. Trans. Telecommun.*, vol. 9, pp. 155-172, Mar. 1998.
- [6] X. Li, A. Chindapol, and J. A. Ritcey, "Bit-interleaved coded modulation with iterative decoding and 8PSK signaling," *IEEE Trans. Commun.*, vol. 50, pp. 1250-1257, Aug. 2002.
- [7] F. Simoens, H. Wymeersch, H. Bruneel, and M. Moeneclaey, "Multi-dimensional mapping for bit-interleaved coded modulation with BPSK/QPSK signaling," *IEEE Commun. Lett.*, vol. 9, pp. 453-455, May 2005.
- [8] S. S. Pietrobon, R. H. Deng, A. Lafanechere, G. Ungerboeck, and D. J. Costello, "Trellis-coded multidimensional phase modulation," *IEEE Trans. Inform. Theory*, vol. 36, pp. 6389, Jan. 1990.
- [9] N. Gresset, J. J. Boutros, and L. Brunel, "Multidimensional mappings for iteratively decoded BICM on multiple-antenna channels," *IEEE Trans. Inform. Theory*, vol. 51, pp. 3337-3346, Sept. 2005.
- [10] N. H. Tran and H. H. Nguyen "Design and performance of BICM-ID systems with hypercube constellations," *IEEE Trans. Wireless Commun.*, vol. 5, pp. 1169-1179, May 2006.
- [11] N. H. Tran and H. H. Nguyen "A novel multi-dimensional mapping of 8-PSK for BICM-ID," *IEEE Trans. Wireless Commun.*, vol. 6, pp. 1133-1142, Mar. 2007.
- [12] H. M. Navazi and Md. J. Hossain, "Efficient multi-dimensional mapping using QAM constellations for BICM-ID," *IEEE Trans. Wireless Commun.*, vol. 16, pp. 8067-8076, Dec. 2017.
- [13] M. Lamarca, H. Lou, and J. Garcia-Frias, "Random labeling: a new approach to achieve capacity in MIMO quasi-static fading channels," *2006 IEEE International Symposium on Information Theory, Seattle, WA*, pp. 1959-1963, 2006.
- [14] M. C. Valenti, R. Doppalapudi, and D. Torrieri, "A genetic algorithm for designing constellations with low error floors," *42nd Annual Conf. on Inf. Sc. and Sys.*, pp.1155-1160, Mar. 2008.
- [15] Y. Huang and J. A. Ritcey, "Optimal constellation labeling for iteratively decoded bit-interleaved space-time coded modulation," *IEEE Trans. Inform. Theory*, vol. 51, pp. 1865-1871, May 2005.
- [16] R. Y. S. Tee, R. G. Maunder, and L. Hanzo, "EXIT-chart aided near-capacity irregular bit-interleaved coded modulation design," *IEEE Trans. Wireless Commun.*, vol. 8, pp. 32-37, Jan. 2009.
- [17] S. T. Brink, "Convergence behavior of iteratively decoded parallel concatenated codes," *IEEE Trans. Commun.*, vol. 49, pp. 1727-1737, Oct. 2001.

- [18] Z. Liu, K. Peng, T. Cheng, and Z. Wang, "Irregular mapping and its application in bit-interleaved LDPC coded modulation with iterative demapping and decoding," *IEEE Trans. broadcasting*, vol. 58, pp. 707-712, Sept. 2011.
- [19] Q. Wang, C. Zhang, and J. Dai, "Irregular mapping design for bit-interleaved coded modulation with low complexity iterative decoding," *2016 6th International Conference on Electronics Information and Emergency Communication (ICEIEC)*, pp. 42-45, Beijing, 2016.
- [20] Q. Xie, Z. Yang, J. Song, and L. Hanzo,, "EXIT-Chart-Matching-Aided Near-Capacity Coded Modulation Design and a BICM-ID Design Example for Both Gaussian and Rayleigh Channels," *IEEE Trans. Veh. Tech.*, vol. 62, no. 3, pp. 1216-1227, March 2013.
- [21] F. Schreckenbach, N. Gortz, J. Hagenauer, and G. Bauch, "Optimized symbol mappings for bit-interleaved coded modulation with iterative decoding," *IEEE Global Telecommunications Conference (GLOBECOM'03)*, vol. 6, pp. 3316-3320, Dec. 2003, San Francisco, CA, USA.
- [22] A. Chindapol and J. A. Ritcey, "Design, analysis, and performance evaluation for BICM-ID with square QAM constellations in Rayleigh fading channels," *IEEE J. Select. Areas Commun.*, vol. 19, pp. 944-957, May 2001.
- [23] N. H. Tran and H. H. Nguyen, "Signal mappings of 8-ary constellations for bit interleaved coded modulation with iterative decoding," *IEEE Trans. Broadcasting*, vol. 52, pp. 92-99, Mar. 2006.
- [24] H. M. Navazi and H. H. Nguyen, "A novel and efficient mapping of 32-QAM constellation for BICM-ID systems," *Springer; Wireless Personal Communications*, vol. 79, pp. 197-210, Jun. 2014.
- [25] H. M. Navazi and Md. J. Hossain, "A novel symbol mapping method for BICM-ID systems for higher order signal constellations," *IEEE Commun. Lett.*, vol. 18, pp. 1323-1326, Aug. 2014.
- [26] L. R. Bahl, J. Cocke, F. Jelinek, and J. Raviv, "Optimal decoding of linear codes for minimising symbol error rate," *IEEE Trans. Inf. Theory*, vol. 20, pp. 284-287, Mar. 1974.
- [27] G. J. Foschini, R. D. Gitlin, and S. B. Weinstein, "Optimization of two-dimensional signal constellations in the presence of Gaussian noise," *IEEE Trans. Commun.*, vol. 22, pp. 2838, Jan. 1974.
- [28] P. K. Viththaladevuni, M. S. Alouini, and J. C. Kieffer, "Exact BER computation for cross QAM constellations," *IEEE Trans. Wireless Commun.*, vol. 4, no. 6, pp. 3039-3050, Nov. 2005.